

FINAL CONTRACT REPORT

**CORROSION PROTECTION SERVICE LIFE OF EPOXY-COATED REINFORCING
STEEL IN VIRGINIA BRIDGE DECKS**

**Michael C. Brown, Ph.D., P.E.
Research Scientist
Virginia Transportation Research Council**

**Richard E. Weyers, Ph.D., P.E.
Charles E. Via, Jr. Professor
Charles E. Via, Jr. Department of Civil and Environmental Engineering
Virginia Polytechnic Institute and State University**

Project Manager
Michael M. Sprinkel, P.E.
Associate Director
Virginia Transportation Research Council

Contract Research Sponsored by
Virginia Transportation Research Council

Virginia Transportation Research Council
(A Cooperative Organization Sponsored Jointly by the
Virginia Department of Transportation and
the University of Virginia)

Charlottesville, Virginia

September 2003
VTRC 04-CR7

NOTICE

The project that is the subject of this report was done under contract for the Virginia Department of Transportation, Virginia Transportation Research Council. The contents of this report reflect the views of the authors, who are responsible for the facts and the accuracy of the data presented herein. The contents do not necessarily reflect the official views or policies of the Virginia Department of Transportation, the Commonwealth Transportation Board, or the Federal Highway Administration. This report does not constitute a standard, specification, or regulation.

Each contract report is peer reviewed and accepted for publication by Research Council staff with expertise in related technical areas. Final editing and proofreading of the report are performed by the contractor.

Copyright 2003 by the Commonwealth of Virginia

ABSTRACT

The corrosion protection service life extension provided by epoxy-coated reinforcement (ECR) was determined by comparing ECR and bare steel bars from 10 Virginia bridge decks built between 1981 and 1995. The objective was to determine the corrosion protection service life time extension provided by ECR field specimens with various degrees of coating adhesion: disbonded, partially disbonded, and wholly bonded coatings.

The size and length distributions of cracks in Virginia bridge decks were investigated to assess the frequency and severity of cracks. Correlation of cracks with chloride penetration was used to characterize the influence of cracking on deck deterioration. Cracks influence the rate of chloride penetration, but the frequency and width distributions of cracks indicate that cracks are not likely to shorten the overall service life of most bridge decks in Virginia.

Altogether, 141 drilled cores, 102 mm (4 inches) in diameter, were employed in this study. For each of the decks built with ECR, 10 to 12 cores were drilled through a top reinforcing bar adjacent to the previous study core locations. In addition, approximately 3 cores were drilled through a top reinforcing bar at a surface crack location. Laboratory testing involved nondestructive monitoring using advanced electrochemical techniques to periodically assess the corrosion state of the steel bars during cyclic exposure to chloride-rich solution over 36 months of treatment. Time of corrosion initiation and time of cracking (where applicable), as well as chloride content of the concrete before and after treatment, were used in the analysis. Analysis of the epoxy coating after treatment showed the presence of micro cracks in the surface of some coatings, and moisture uptake and glass transition temperatures, as related to curing of the coatings, were investigated.

Less than 25 percent of all Virginia bridge decks built under specifications in place since 1981 is projected to corrode sufficiently to require rehabilitation within 100 years, regardless of bar type. The corrosion service life extension attributable to ECR in bridge decks was found to be approximately 5 years beyond that of bare steel and, therefore, ECR is not a cost-effective method of corrosion prevention for bridge decks. Virginia would save approximately \$845,000 per year in bridge deck construction costs by deleting the requirement for ECR.

FINAL CONTRACT REPORT

CORROSION PROTECTION SERVICE LIFE OF EPOXY-COATED REINFORCING STEEL IN VIRGINIA BRIDGE DECKS

Michael C. Brown, Ph.D., P.E.
Research Scientist
Virginia Transportation Research Council

Richard E. Weyers, Ph.D., P.E.
Charles E. Via, Jr. Professor
Charles E. Via, Jr. Department of Civil and Environmental Engineering
Virginia Polytechnic Institute and State University

INTRODUCTION

The Bridge Division of the Federal Highway Administration maintains the National Bridge Inventory, a database of highway bridges throughout the United States that are 6 meters (20 feet) or more in length. Bridges that are considered inadequate for current or projected use are classified as either structurally or functionally deficient. Structurally deficient bridges are those designated as needing significant maintenance attention, rehabilitation, or replacement. The National Transportation Statistics Report for 1999 states that in 1990, from a total of 572,205 rural and urban bridges over 24% (137,865) were considered structurally deficient (National Transportation Statistics 1999, 2000). A significant percentage of such deficiencies are due to reinforcing steel corrosion as a result of marine environment or deicing salt exposure.

A memorandum circulated within the Virginia Department of Transportation indicated that Virginia has a total of approximately 25 million square feet of bridge deck within 4,432 bridge structures that are eligible for maintenance replacement funding based on age and condition. Of this figure, 794 Virginia structures, comprising almost 14.7 million square feet of bridge deck, were considered part of the National Highway System (NHS) bridge inventory (Kerley, M., 1998).

In 1998, rehabilitation and replacement expenditure requirements for Virginia bridge decks were projected to be \$150 million. NHS structures accounted for nearly half, or \$70 million, of the predicted rehabilitation costs. Meanwhile, an estimated \$1.4 billion in costs was forecast for replacement of aged and structurally deficient bridges, of which NHS structures accounted for about \$400 million dollars, or nearly 30%. These anticipated expenditures were above and beyond the costs of routine maintenance and inspection, which average over \$10 million and \$7 million per year, respectively (Kerley, M., 1998).

It is clear that the Virginia Department of Transportation must address the growing need for maintenance and rehabilitation funding, in the face of shrinking revenues. Thus, funded research has focused on corrosion prevention alternatives and life-cycle prediction for corrosion-related damage to Virginia bridge structures, in an effort to make informed decisions about rehabilitation and replacement alternatives.

PURPOSE AND SCOPE

Information about service life, life-cycle costs and anticipated time to repair, rehabilitation, and/or replacement of bridge decks built with ECR would be useful to practicing bridge engineers and maintenance personnel. The purpose of the study was to compare ECR and bare steel bars from bridge decks built between 1981 and 1995 to determine the corrosion protection service life time extension provided by ECR field specimens with various degrees of coating adhesion: disbonded, partially disbonded, and wholly bonded coatings.

The scope of the research was limited to the sampling, preparation and testing of a series of concrete cores containing bare steel from 2 bridge decks, and ECR from 8 bridge decks. The samples were used in a laboratory investigation to assess the corrosion-related service life of ECR compared to bare steel. Laboratory testing involved nondestructive monitoring using advanced electrochemical techniques to periodically assess the corrosion state of the steel bars during cyclic exposure to chloride-rich solutions over 36 months of treatment. The chloride content of truncated specimens was assessed at the time treatment was terminated. Time of corrosion initiation and time of cracking (where applicable), as well as chloride content of the concrete before and after treatment, were used in the analysis.

BACKGROUND

In the late 1960s, corrosion of reinforcing steel in concrete bridges became a central point of concern in North America, as many bridges were in need of repair after only a few years of service (Manning, D. G., 1996). The rapid deterioration was attributed to the increased use of deicing salts (Cady, P. D., 1977). Swift improvements were made to increase concrete quality, depth of clear concrete cover, and to tighten quality assurance procedures. However, further research was deemed necessary for a long-term method of addressing reinforcing steel corrosion (Manning, D. G., 1996).

In 1972, the Federal Highway Administration (FHWA) and National Bureau of Standards (NBS, now National Institute of Standards and Technology, NIST) began a feasibility study of organic coatings to protect reinforcing steel in concrete bridge decks (Clear, K. C. et al., 1995; Weyers, R. E., 1995). By 1976, within four years of the placement of epoxy coated reinforcement (ECR) in the first test bridge deck in Pennsylvania, over 40 bridges in the U.S. had incorporated the material (Manning, D. G., 1996; Weyers, R. E., 1995). Epoxy coatings on steel became the prevalent corrosion prevention method by 1981.

In 1986, premature corrosion deterioration in 6-year-old bridge substructure components in the Florida Keys sparked a new debate over the long-term performance of ECR (Sagüés, A. A. et al., 1994). As a result, studies in recent years have begun to question the long-term performance of epoxy coating systems toward corrosion prevention. Further work has been conducted by various state departments of transportation and independent researchers to characterize the life expectancy of structures built with ECR in a variety of climates.

Meanwhile, some states, such as Florida and Oregon, have discontinued use of ECR altogether as an option for design and construction in coastal regions (Manning, D. G., 1996; Covino, B. S. et al., 2000).

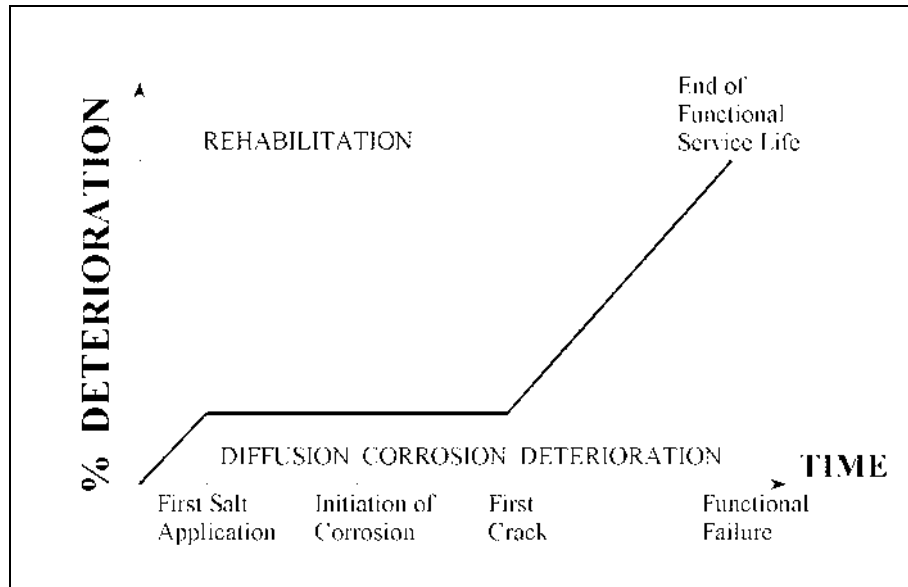


Figure 1 Service Life Model for Chloride-Induced Corrosion of Reinforced Concrete

Figure 1 illustrates a general service life model for reinforced concrete undergoing corrosion-related deterioration. Arguably, ECR has the same chloride initiation concentration at bare locations (coating damage, holidays, and imperfections) as that of uncoated bars. This is supported by McDonald and others, who stated, "Half-cell potentials obtained for the damaged epoxy-coated bars were similar to that determined for black steel. Based upon this review, it was determined that the chloride threshold for damaged epoxy-coated bars is similar to that of black bars"(McDonald, D. B. et al., 1998). Therefore, the ECR service-life extension period will result from variations in the rate of metal dissolution and accumulation of corrosion product, and resultant differences in pressure being generated by the corrosion products over time during the active corrosion period.

METHODS AND MATERIALS

The study involved field sampling of bridge decks built with ECR and bare steel, followed by preparation of the specimens prior to cyclic exposure to a chloride solution and electrochemical monitoring in the laboratory. Analysis of the relative corrosion response of ECR and bare steel specimens to cyclic chloride exposure provided an indication of the service life extension to be expected of the ECR system. The experimental procedures involved laboratory assessment of ECR specimens from a subset of 8 bridge decks from the previous study (Pyc, W., 1998) and 2 bridge decks with bare steel (uncoated) bars.

Field Survey and Sampling

Bridge Deck Selection

The decks were selected based upon relative adhesion rating and diffused chloride content, as determined in a previous study (Pyc, W., 1998). Two bridge decks were sampled from each of four ranges of dry knife adhesion rating. In addition, two bridge decks constructed with bare steel bars, but constructed within the same time period as the ECR bridges and thus under the same concrete and cover depth specifications, were sampled and used as controls. Deck selection information is provided in Table 1 and Figure 2 presents the location of the bridge structures. The presented deck age is the age at sampling.

Table 1 Selection of ECR and Bare Steel Bridge Decks (Pyc, W., 1998)

District	Structure Number	Year Built	Age (yrs)	Average Adhesion	Average Chlorides @ 13 mm, (kg/m ³)*
3	1004	1983	16	1.0	4.5
1	1136	1995	4	1.0	1.4
9	2262	1985	14	1.5	2.2
2	1015	1987	12	2.5	5.8
7	1001	1992	7	3.0	2.5
5	2021	1981	18	3.5	1.1
6	1004	1993	6	4.0	0.8
7	1019	1990	9	4.5	1.7
2	6128	1984	18	Bare Steel	-
1	6037	1983	16	Bare Steel	-

* Decks containing bare steel were unique to the current study. No previous data was available.

Sampling Plan

Altogether, 141 drilled cores, 102 mm (4 inches) in diameter, were employed in this study. For each of the decks built with ECR, ten to twelve cores were drilled through a top reinforcing bar adjacent to core locations of the previous study. Core locations were representative of the 12-percentile shallowest concrete cover depth of each span. In addition, approximately three cores were drilled through a top reinforcing bar at a surface crack location. Specific quantities of cracked and uncracked core samples for each deck are detailed in Table 2.

Upon coring, each specimen was allowed to air dry only long enough for surface moisture to evaporate. The samples were then wrapped in multiple layers of polyethylene sheet, aluminum foil, and duct tape to maintain as closely as practical the in-place moisture condition of the concrete during transport and storage.

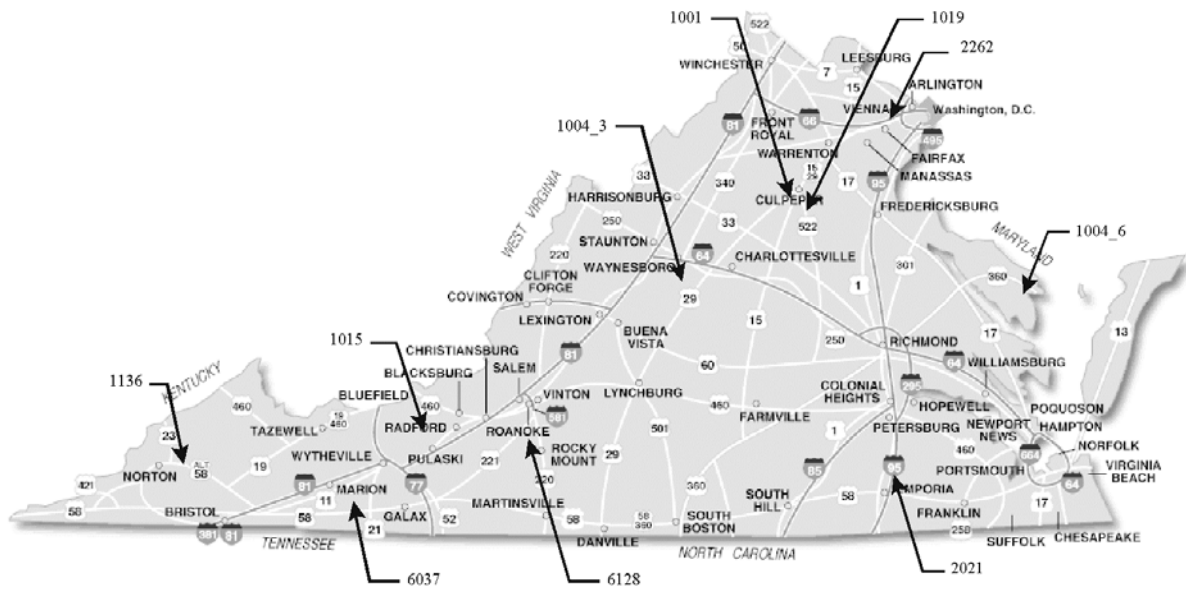


Figure 2 Selected Bridge Locations

Field Evaluation

In addition to obtaining cores, as indicated above, additional information about bridge deck condition was obtained. A sounding survey, using chain drag and hammer, was conducted to identify delaminated areas, and visible spalls were noted. Powdered concrete samples were obtained using a hammer-drill and sampling bit, with attached filter collection device, at 13 mm depth increments from 6 mm to 71 mm, in three locations per bridge adjacent to cores containing identified surface cracks. Powdered concrete samples were used for chloride concentration profiles and diffusion analyses.

The field survey was limited to the right travel lane because field experience has shown that this lane most often deteriorates first. The field survey of each deck consisted of 40 clear cover depth readings on each span and a visual linear crack survey. The crack survey consisted of the number and length of cracks in each span, categorizing them as either longitudinal, transverse, or diagonal relative to the direction of traffic. Transverse and diagonal cracks were considered together, and differentiated from longitudinal cracks. Very few diagonal cracks were observed. Surface crack widths were measured visually with a crack comparator, generally at one-foot intervals along each crack. However, in all cases, no less than 5 crack widths were measured for a crack.

Laboratory Testing

All cores were visually examined for surface cracks. Cores that were taken in the field in visibly uncracked sections (crack widths < 0.08 mm were not visible in the field), but later discerned to contain surface cracks, were also considered cracked. Crack widths and depths were measured, noting whether or not the crack extended to the depth of the reinforcing steel.

Sample Treatment and Exposure

Each core obtained from field sampling was divided into several parts for use in determining chloride and moisture content and subsequent laboratory corrosion assessment using electrochemical and visual techniques.

Core Preparation Procedure

For each core, the section of concrete 13 mm ($\frac{1}{2}$ inch) above the reinforcing steel was removed by dry sawing. Concrete chloride content, moisture content, percent absorption and percent saturation were determined for two 13-mm ($\frac{1}{2}$ -inch) sections. Chloride contents were measured at two depths; one 13 mm below the surface and the other 19 mm above the reinforcing bar. Acid-soluble chloride concentrations were measured in crack sections and adjacent uncracked sections. A diagram of core sectioning is presented in Figure 3, which presents the location of the chloride samples taken from field cores. For some sample locations, depending upon depth of clear cover, chloride samples may not have been obtained at certain depths.

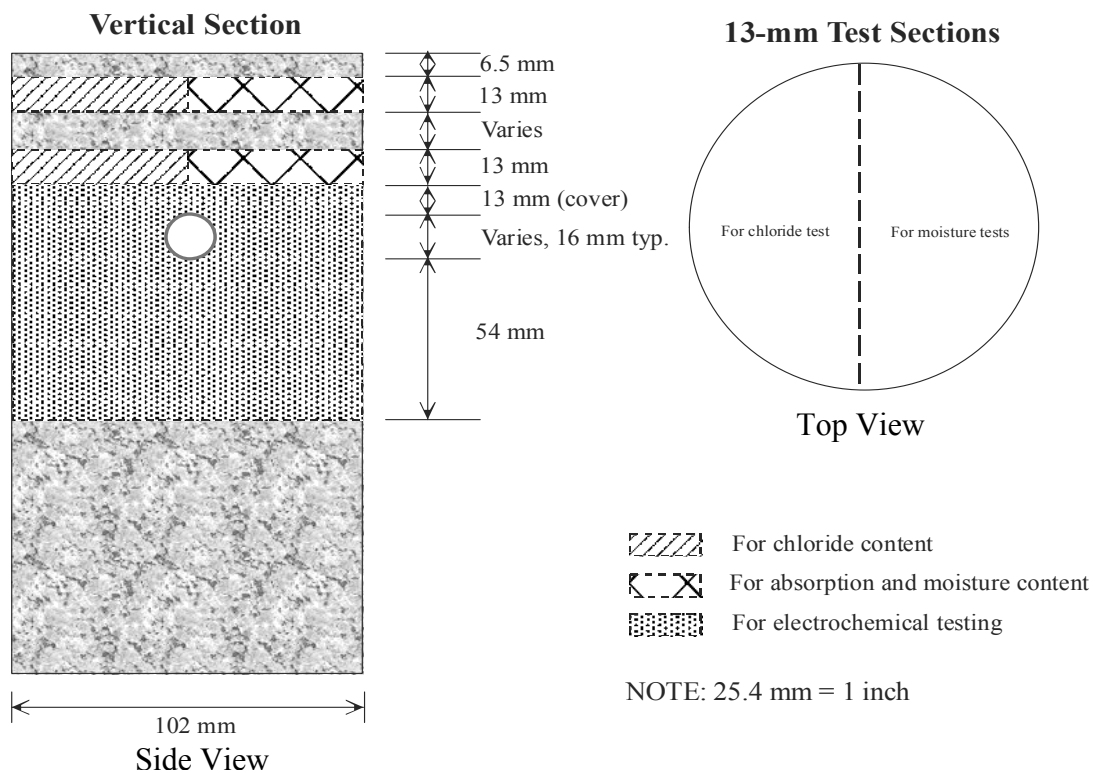


Figure 3 Core Section Plan

Cores containing vertical cracks were evaluated differently. In general, chloride samples from cracked concrete sections were 19 mm wide, 13 mm thick, and 100 millimeters long and centered over the crack as shown in Figure 4. The samples were crushed to pass a #20 sieve, and sampled for chemical analysis. In addition, chloride contents were measured in sections of the core away from the crack.

Dry saw-cutting and specimen preparation was conducted in groups by bridge, resulting in 10 groups. After the specimens were unwrapped, visual and photographic documentation of cores was accomplished. Exposed steel bar ends were cleaned and samples were obtained from the appropriate depths of the core by dry saw-cutting. Samples were obtained for chloride and moisture determination and sections containing the reinforcement bar were prepared for laboratory exposure to chloride solution and monitoring.

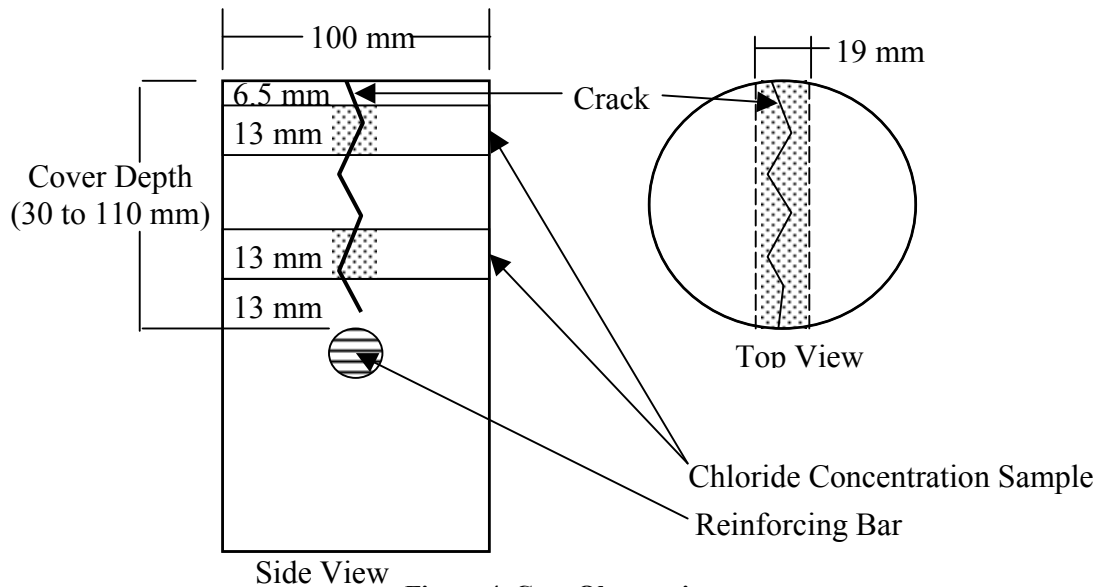


Figure 4 Core Observation

One end of the reinforcing bar was drilled and tapped (dry) and a stainless steel screw was inserted. The perimeter and bottom of the specimen were coated with paraffin wax, and the top remained exposed. A section of PVC pipe, 76-mm (3-inch) i.d., was fixed to the top of the core and sealed with silicone sealant to create a ponding reservoir. The reduced diameter of the ponding dike was used to create a longer path of diffusion and migration for chloride to the ends of the bars at the core perimeter, which are more susceptible to corrosion (see Figure 5).

The length of core below the bar was kept constant at 54 mm for all specimens, where possible. Timing of core preparation and subsequent testing was staggered, with specimens divided into two to four major groups on alternate ponding cycles, to allow most efficient use of the electrochemical analysis equipment.

After preparation, the concrete core specimens were ponded with 3% NaCl solution. Chloride solution exposure was cycled on a weekly basis, by ponding for 2 days, followed by 3 to 5 days of drying under laboratory conditions, depending upon whether monthly testing was due for a given specimen. Testing occurred immediately after ponding solution was removed to assure good conductivity of the concrete cover.

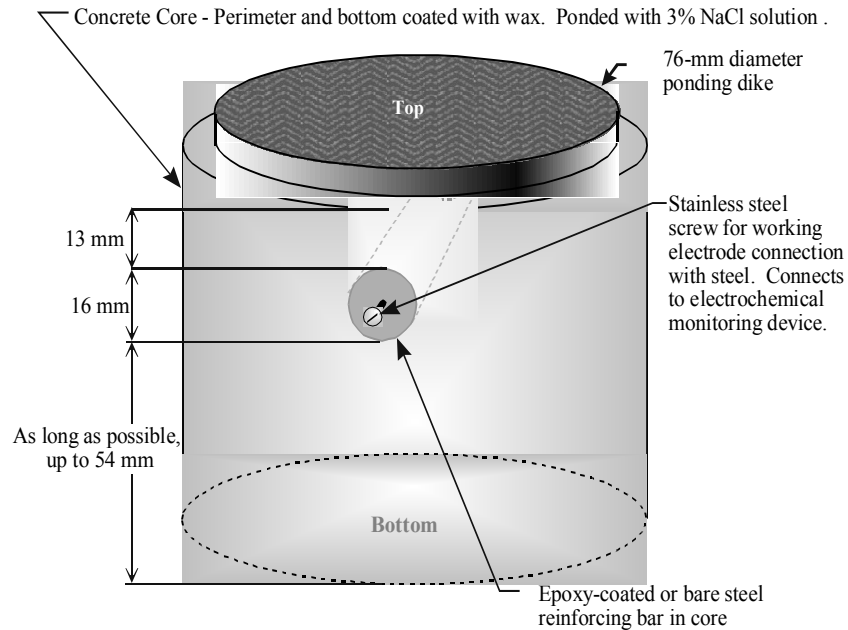


Figure 5 Specimen with Ponding Reservoir

Laboratory Tests

Moisture Content

Moisture samples were weighed immediately after cutting. Percent absorption, and percent saturation of two 13-mm ($\frac{1}{2}$ -inch) sections, centered at 19 mm ($\frac{3}{4}$ inch) above the ECR bars and 10 mm ($\frac{3}{8}$ inch) from the surface, respectively, were determined in general accordance with ASTM C 642-97 (ASTM, 1997). One exception involved individual smaller sample size than recommended by the method. However, the precision of the mass determinations far exceeded the precision criterion. Initial percent saturation was estimated using the initial weight measurements in conjunction with absorption data from the test.

Chloride Tests

Concrete sub-samples were pulverized and ground to a powder using rock-crushing equipment and mortar and pestle until it passed the #20 sieve. Acid soluble chloride content was measured in accordance with ASTM C 1152-90 (ASTM, 1990).

Chloride tests were also performed on powdered concrete samples obtained from the deck by drilling with a hollow-bore impact bit adjacent to cores containing cracks. The drill bit diameter was 29 mm (1.125 inches) and thus 1.5 times the maximum coarse aggregate size of 19 mm ($\frac{3}{4}$ inch). Apparent chloride diffusion constants were calculated from the 13-mm increment powdered concrete profiles. The chloride concentration from 58 mm to 71 mm depth, which did not appear to be influenced by chloride ingress from the environment, was considered the nominal background chloride content. All measured chloride concentrations from a given bridge were then adjusted by subtracting the average value from the three deepest powdered concrete determinations, to reveal the concentration of "diffused" chloride.

Corrosion progress and coating properties were monitored using Electrochemical Impedance Spectroscopy (EIS). The major components of the test system included a computer-operated potentiostat and appropriate software. The Gamry Instruments PC3/300 Potentiostat / Galvanostat / ZRA system of integrated circuit cards for use in IBM-PC compatible computers was employed, along with the associated Framework software. The user interface and control of the PC cards and selection and manipulation of electrochemical techniques was coordinated through the Framework software, and analysis was performed via spreadsheets.

Custom probes were fabricated for use in the electrochemical tests to accommodate the new ponding reservoir. Each probe consists of a titanium mesh counter-electrode cut to 63-mm (2½-inch) diameter and sandwiched in an open cell sponge to maximize electrical surface contact. The sponge assembly was attached to a probe housing fabricated to accommodate a pen-cell type saturated Cu/CuSO₄ (CSE) half-cell reference electrode. A small concrete weight was cast for each probe to enhance surface contact. Figure 6 is a schematic of a typical core specimen with connections and probe for EIS testing.

To permit efficient EIS testing of the prepared samples containing epoxy coated or reference bare steel bars, two multiplexed electrochemical testing systems were used. The two systems, based on Gamry Instruments Model PC3/300 potentiostats installed in separate IBM compatible personal computers, were each linked to a Gamry ECM8 eight-channel multiplexer. The two systems, running in parallel, each perform potentiostatic EIS measurements on eight specimens, to be tested consecutively over a one- to two-day period.

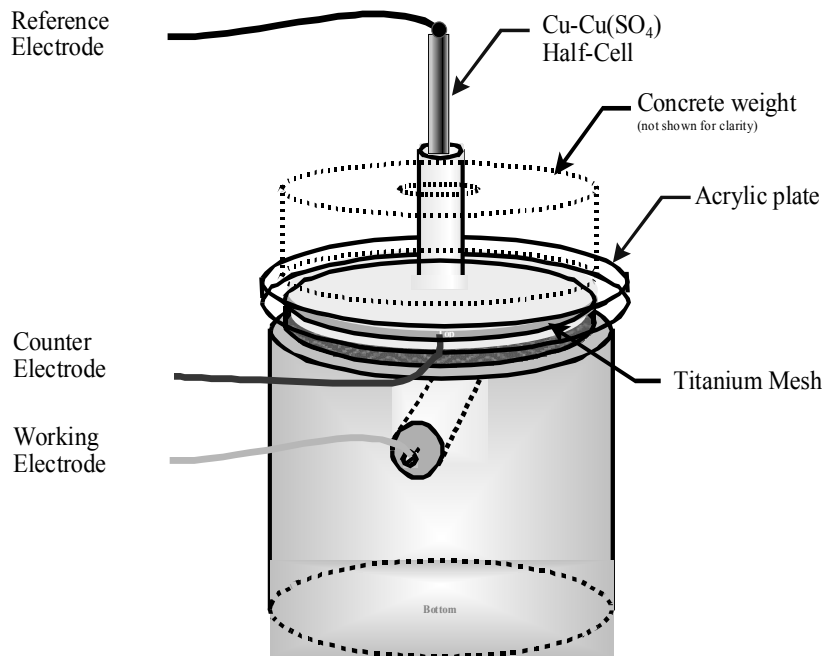


Figure 6 Test Probe and Cell Connections Design

After an initial potential scan to assure electrochemical stability, EIS was performed using a frequency range of 0.001 Hertz to 5000 Hertz with ± 10 mV RMS amplitude about the corrosion potential. The two multiplexed EIS systems, running in parallel, performed potentiostatic EIS over the selected frequency spectrum on a total of sixteen specimens in a 24-hour period. The preparation of specimens was performed in ten groups of sixteen specimens. The preparation occurred at two-day intervals over a four-week period. After preparation and curing of sealant, an EIS test was performed on each specimen prior to initiation of ponding with 3% NaCl. The specimens were then subject to a regular ponding cycle, including two days of ponding, and five days of drying under room temperature and relative humidity conditions each week. During every fourth week, immediately following ponding, the specimens were subject to EIS tests over one to two days and then the dry period was limited to three to four days. Ponding cycles for the specimens were divided into three major groups, to stagger the testing cycle as appropriate for three groups of up to sixteen tests per week. All 141 specimens were prepared and tested in approximately four weeks. The specimens were subsequently tested at four-week intervals.

Post-cracking evaluation

Post-cracking observations of the cyclically ponded cores included documentation of the width, length, and orientation of the crack at the core surface. The core was then dry-cut in accordance with Figure 7 to permit visual observation and extraction of the reinforcement bar, as well as sampling of concrete adjacent to and above the site of active corrosion.

Adhesion rating

Immediately after exposure, the reinforcement was photographed, along with the bar trace of the surrounding concrete, to document the physical condition. For ECR samples, a knife adhesion test was performed, using the same criteria applied in a previous study (Pyc, W. A. et al., 2000). The adhesion rating was documented for six locations on each bar; three on the top and three on the bottom. In addition, the color of the bar surface beneath the coating was documented, also using similar ratings to those employed in the previous study. The adhesion and color rating results were also photographically documented.

Chloride analysis

Samples of concrete adjacent to and directly above the site of active corrosion along the bar were crushed to pass a # 20 sieve and subject to acid-soluble chloride concentration tests in accordance with ASTM C 1152-90. These values were taken to indicate the concentration of chloride at the corrosion site at the time of cracking. As before, values were adjusted by subtracting the nominal background chloride content of the concrete in the bridge. Samples were generally greater than 10.0 g, as specified, but a few samples were slightly less, depending upon the dimensions of the core, orientation of the reinforcing bar and the size of the active corrosion site.

Truncated Observations

After approximately 22 months of exposure, 27 of 28, or 96%, of the bare steel specimens had cracked and been subject to destructive assessment. Since only 21 of 113, or

19%, of ECR specimens had cracked at this time, more information was desired about the distribution of diffused chlorides in the remaining ECR cores. A group of 17 cores was selected at random from among all the remaining ECR cores. This group represented a set of "truncated observations," in which the post-cracking evaluation procedures were applied, even though a visible crack had not yet been identified. The observed bar condition, coating condition, and chloride contents for each specimen were then used to surmise the status of the remaining ECR cores. After 36 months of exposure, 30 additional cores were selected at random for truncation; 15 had initiated corrosion, and 15 had not initiated corrosion. Thus, 66 of the original 113 ECR specimens were allowed to proceed through the point of cracking or remain un-cracked and have not received post-cracking evaluation after treatment ceased.

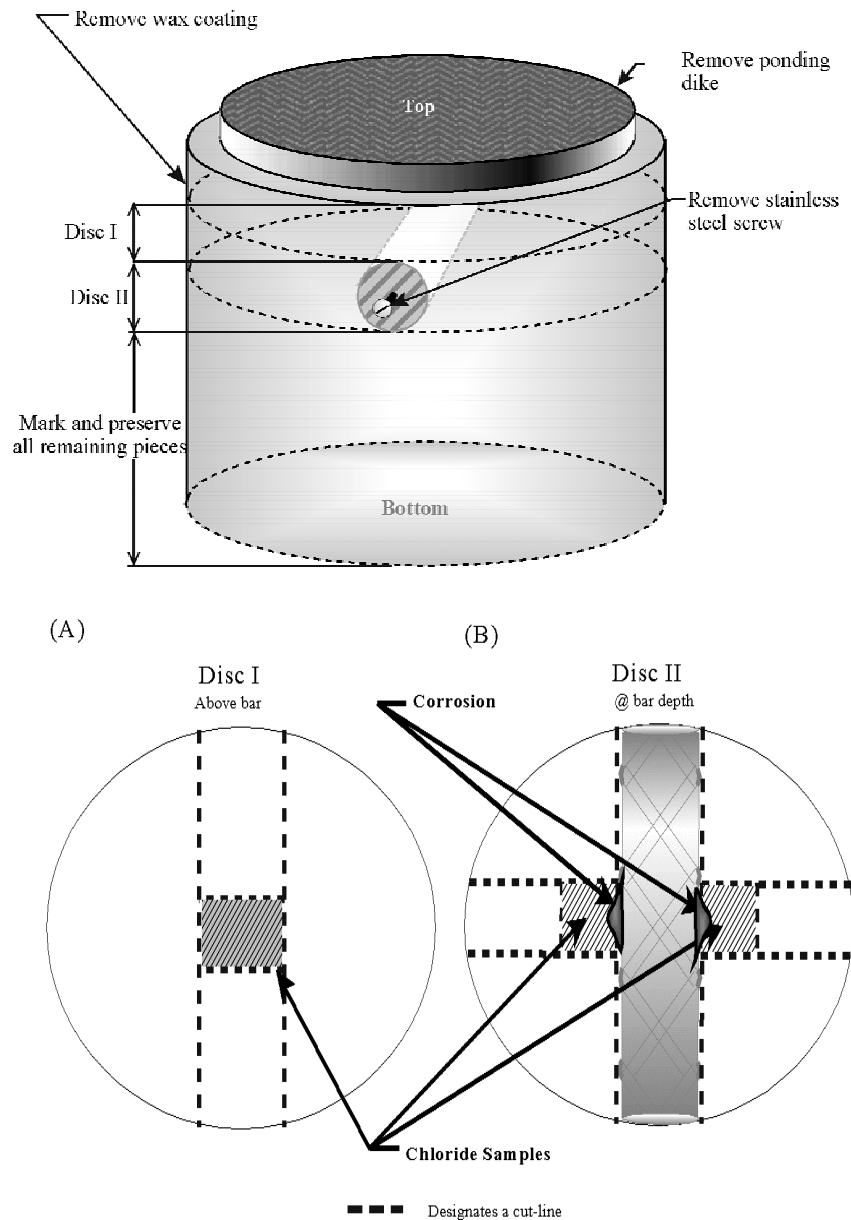


Figure 7 Post-cracking Sampling Plan for Laboratory Specimens

RESULTS

Although the plan called for 15 cores from each deck, the exact number of cores with and without surface cracks varied based on field conditions. Table 2 presents the district bridge designations, route locations, ages at sampling, and exact numbers of samples from each deck.

Table 2 Core Sample Classification

Structure Number	District-County	Route	Year Built	Age at Sampling	Total Number of Cores	Uncracked Cores	Cores Containing Surface Cracks
1136	1 - Wise	SR 72	1995	4	15	11	4
1004.6	6 - Northumberland	SR 200	1993	6	13	9	4
1001	7 - Culpeper	US 29	1992	7	14	11	3
1019	7 - Culpeper	US 522	1990	9	13	8	5
1015	2 - Giles	SR 100	1987	12	14	10	4
2262	9 - Fairfax	Vaden Drive	1985	14	15	10	5
6128	2 - Franklin	County 740	1984	15	16	11	5
1004.3	3 - Nelson	SR 6	1983	16	14	11	3
6037	1 - Grayson	County 662	1983	16	12	10	2
2021	5 - Greensville	I-95	1981	18	15	10	5
Total					141	101	40

Table 3 presents respective Virginia Engineering District, dates of construction and age at the time of the survey, number and length of spans, superstructure type, and reinforcing steel type for all bridges in the study. The bridges were built between 1981 and 1995 and were 4 to 18 years of age at the time of the field survey. Bridge superstructures were primarily simply supported or continuous design steel girder systems with composite decks. One structure was prestressed concrete I-beams with continuous span design. Previous research has shown that transverse cracking is more frequent for steel girders and more frequent for continuous girders than simply supported girders (Krauss, P. D. & Rogall, E. A., 1996).

Table 3 Bridge Superstructure Type and Reinforcing Steel Type

District	Structure Number	Year Built	Age at Sampling (yrs)	No. Spans	Span Lengths (m)	Superstructure Type	Reinforcing Type
1-Bristol	1136	1995	4	3	22/22/22	S/C	ECR
6-Fredericksburg	1004	1993	6	3	13/13/27	PI/C	ECR
7-Culpeper	1001	1992	7	3	23/23/24	S/C	ECR
7-Culpeper	1019	1990	9	3	15/26/15	S/S	ECR
2-Salem	1015	1987	12	3	15/24/15	S/S	ECR
9-Northern VA	2262	1985	14	4	21/20/25/23	S/S	ECR
1-Bristol	6037	1983	16	2	20/20	S/S	BS
3-Lynchburg	1004	1983	16	3	18/18/19	S/C	ECR
2-Salem	6128	1981	18	2	17/17	S/S	BS
5-Suffolk	2021	1981	18	3	21/21/21	S/C	ECR

S/S: steel girders, simply supported S/C: steel girders, continuous design
 PI/C: prestressed I-beams, continuous design ECR: epoxy coated reinforced steel
 BS: bare reinforcing steel

Span lengths were generally equivalent, with the shortest span of 13 m and the longest span of 27 m, both on Fredericksburg structure No. 1004. The two bare steel decks were 15 and 16 years old when the field survey was conducted. These bridges are among the oldest bridges surveyed, as construction with bare steel reinforcement was discontinued when ECR was accepted into common use. These two bridges are in the highest snowfall area of the state, but are located on County Routes, which have lower traffic counts than U.S. and Interstate routes.

Influence of Cracking

Field Survey

Table 4 presents the total longitudinal and transverse/diagonal cracks for average crack width of less than and equal to 0.30 mm and greater than 0.30 mm. As shown, the total length of longitudinal cracks is significantly greater than the total length of transverse/diagonal cracks, 1109 m and 172 m, respectively. Also, the greater percentages of the longitudinal and transverse cracks were less than 0.30 mm, 85 and 95 percent, respectively. The total length of cracks is less for the bare steel than any of the ECR decks. However, the subset of BS decks was too small to allow conclusions as to the influence of steel type.

Table 4 Bridge Survey Area and Crack Length

Survey Age (years)	Survey Area (m ²)	Crack Length (mm)			
		Longitudinal		Transverse/Diagonal	
		Width ≤ 0.30mm	Width > 0.30mm	Width ≤ 0.30mm	Width > 0.30mm
4	411.7	82.8	7.2	50.9	5.7
6	196.2	77.4	1.6	40.9	0.0
7	312.5	94.2	0.0	38.6	1.2
9	347.5	165.1	29.1	22.8	0.9
12	359.5	25.8	25.8	0.0	0.0
14	326.6	240.2	4.9	0.0	0.0
16*	285.4	0.0	0.0	0.0	0.0
16	372.0	154.8	41.1	0.0	0.0
18*	254.9	20.0	11.3	9.6	1.4
18	479.9	85.8	42.2	0.0	0.0
Total	3,346.2	946.1	163.2	162.8	9.2
	Percent	85.3%	14.7%	94.7%	5.3%

*Deck contains bare steel reinforcement, others were constructed with ECR.

Cover Depth Survey

Clear cover depths, 40 per span, were averaged to determine the cover depth distribution and were compared to the applicable construction specifications. These data were taken from the preceding study involving 21 bridges, all containing ECR (Pyc, W., 1998). The average clear cover was 65 mm with a standard deviation of 9.1 mm. The average cover depth of the two bare steel bridges in this study was 55 mm and standard deviation was 11.5 mm. Overall, field cover depths ranged from 43 mm to 116 mm. The average directly measured clear cover depth from 141 core samples in this study was 69 mm, with a standard deviation of 14.3 mm. The structures

were built under the same concrete specification, with a maximum water-to-cement ratio (w/c) of 0.45 and a cover depth of 63 mm to 76 mm ($2\frac{1}{2}$ to $3\frac{1}{8}$ inches) (Virginia, 1978, 1982, 1987, 1991).

Crack Frequency

The number of longitudinal cracks ranged from 0 to 4 in a span-lane and from 0 to 11 for a deck. The number of transverse/diagonal cracks ranged from 0 to 9 in a span-lane and from 0 to 16 for a deck. For the 8 decks built with ECR, there were 51 longitudinal and 56 transverse/diagonal cracks. Of these decks, 4 span-lanes had no longitudinal cracks and 15 span-lanes had no transverse cracks from the sub-sample of 25 span-lanes. For the two BS decks, there were 6 longitudinal and 5 transverse cracks spread over the 2 span-lanes of structure 6128. Structure 6037 had no longitudinal or transverse/diagonal cracks. The number of transverse and longitudinal cracks does not appear to be a function of span length.

Laboratory Core Evaluations

Crack Width and Depth in Cores

Although only 30 cores in the field were identified with surface cracks and targeted for sampling, several of the cores sampled from what in the field seemed to be uncracked concrete had apparent surface cracks after core sampling. The presence of these cracks, which were oriented vertically in the cores, is not attributed to the coring process, but more likely represents preexisting cracks that were not visible in the rough finished surface. These cracks became apparent after removal from the deck, possibly from the loss of confining pressure from the surrounding concrete. Thus, 40 cores contained cracks and were incorporated in the cracked cores subset for the study.

The crack widths for all the cores that contained a surface crack ranged from 0.08 mm to 0.33 mm and crack depths ranged from 3 mm to 162 mm. Only one of the 40 cores, core 2 from structure 1015, built in 1987, had a surface crack greater than 0.30 mm. Only 7.5% of the cracks in cores were greater than or equal to 0.30 mm in width. Only 5 of the cracks, or approximately 12.5%, penetrated to the depth of the reinforcing steel and all 5 cracks were from the 30 cores deliberately drilled over a crack identified in the field.

Moisture Content

Results of the concrete density, absorption, and percent saturation tests are presented elsewhere (Brown, M. C., 2002). Tests indicate that the concrete specimens, although stored in multiple layers of polyethylene sheet and aluminum foil, likely did lose some moisture between field sampling and laboratory specimen preparation. From 275 determinations, the average moisture content for all specimens was 66% with a standard deviation of 7.8%. The highest average percent saturation for a bridge group was 76% and the lowest average percent saturation was 55%. The moisture content of sections 6 mm to 19 mm below the top surface was not different from that of the sections 13 mm to 26 mm above the reinforcement.

Chloride Content

The acid-soluble chloride content of concrete, extracted from slices of the cores at two depths, was determined by potentiometric titration. The ingress of chloride into concrete bridge

decks is commonly modeled using a solution of Fick's Second Law of Diffusion, as approximated for one-dimensional diffusion into a semi-infinite slab:

$$C_{(x,t)} = C_0 \left(1 - \operatorname{erf} \frac{x}{2\sqrt{D_c t}} \right) \tag{Equation 1}$$

where; $C_{(x,t)}$ = chloride concentration at depth x after exposure time t
 C_0 = constant chloride concentration near the surface
 D_c = effective diffusion coefficient
 erf = mathematical error function (Rieger, P.H., 1994).

The rate of chloride ingress into the concrete is dependent upon the quality of the cement paste, including cement and water content, and degree of maturity, which in turn affect pore size distribution and tortuosity of the capillary pore system. Capillarity has an influence on the system, but is primarily observed in the outer few millimeters of concrete cover, especially for concrete in a saturated or near-saturated condition, as under the cyclic ponding process in this study. The above equation is a simplification of a complex process, and does not consider the influence of chloride binding, leaching, non-homogeneities of aggregate size, shape, and distribution, or variations in saturation and hydration through the depth of the paste matrix, as well as other chemical and physical processes (Sagüés, A. A. et al., 2001; Kranc, S. C. et al., 2002). Therefore, it is recognized that the effective diffusion coefficient employed is not a pure scientific measure, but rather a nominal engineering indicator, which estimates a coefficient, fixed in space and time, to describe the long-term rate of chloride ingress.

Chloride concentrations at the two depths, centered 13 mm (1/2 inch) below surface and 19 mm (3/4 inch) above the surface of the top reinforcing bar, in conjunction with profiles from powdered samples, were used to project the chloride content at each bar depth. A typical chloride profile is shown in Figure 8.

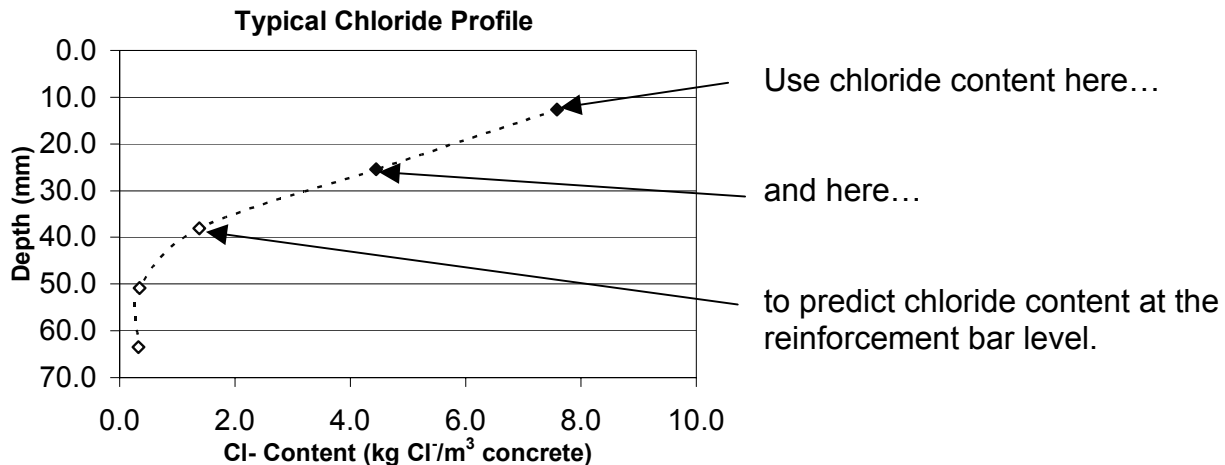


Figure 8 Predicting Chloride Content at the Bar Depth

Analysis of the resulting chloride profiles has been presented elsewhere (Kirkpatrick, T. J., 2001). Figure 9 presents the average and 95% confidence intervals for chloride concentrations at 13 mm depth, assumed to be the driving concentration, C_0 , as a function of age.

C_o was used in conjunction with an apparent field diffusion coefficient, D_c . The resulting estimated average D_c and 95% confidence interval is plotted in Figure 10. A few of the specimens that contained cracks resulted in very high estimated diffusion coefficients. Since these conditions were not solely related to the diffusion process, the samples were removed from the data presented.

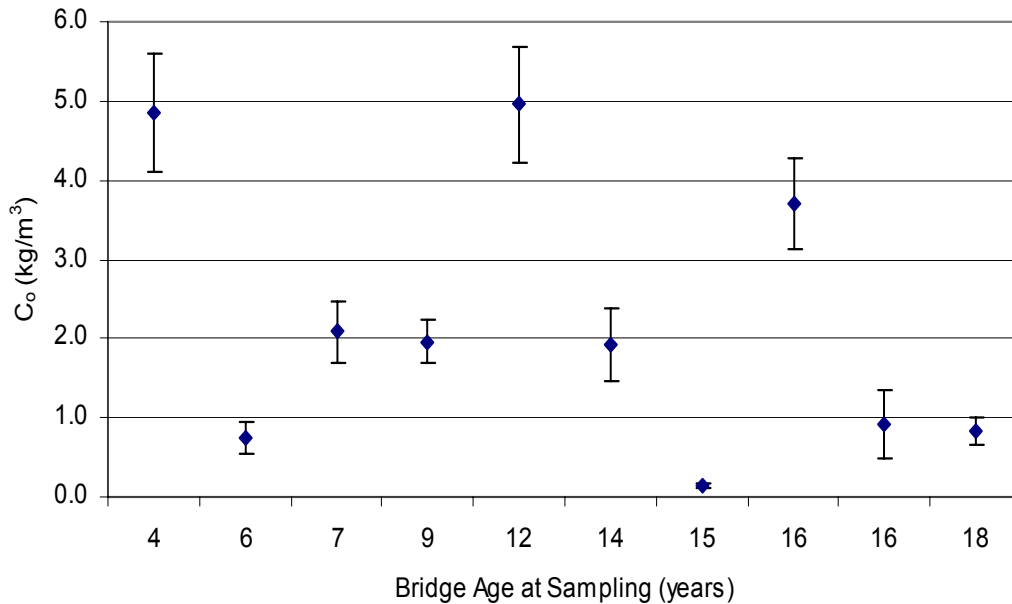


Figure 9 Chloride Diffusion Parameters by Age – Surface Concentration, C_o

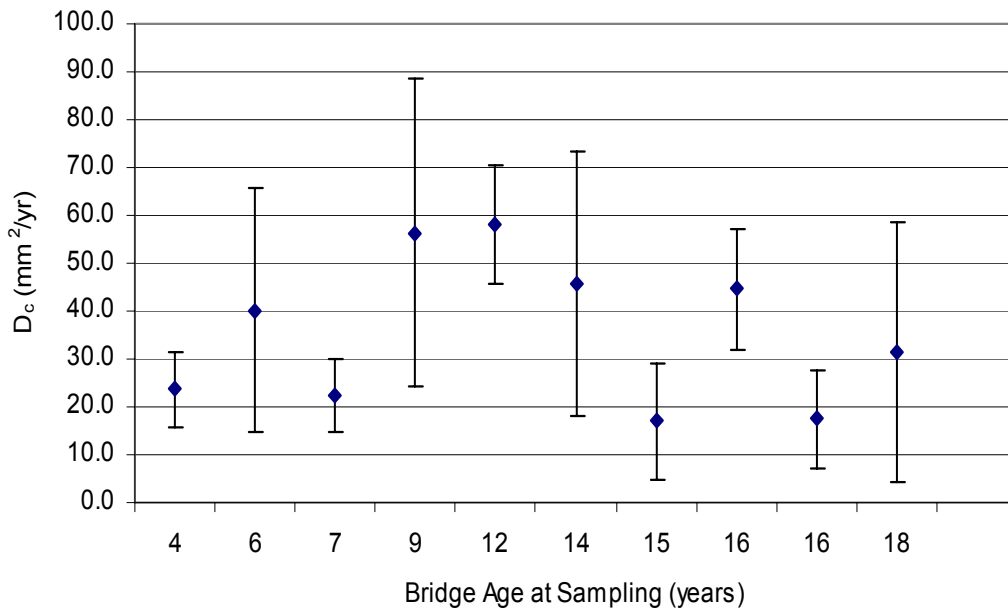


Figure 10 Chloride Diffusion Parameters by Age – Diffusion Coefficient, D_c

Corrosion Potential and Impedance Monitoring

During the laboratory treatment period, the specimens were ponded, and tested periodically to monitor the condition of the coatings and the presence or absence of active corrosion. The open-circuit potential and selected impedance data were compiled and tracked as a function of time. Specifically, the modulus of impedance, as defined previously, and the associated phase angle were recorded at frequencies of 1 mHz, 1 Hz, and 5000 Hz.

Based on previous experience with EIS data for reinforced concrete specimens, the frequencies were selected to give general indications about components of the physical system (Pyc, W. A. et al., 2000). The impedance at 5000 Hz is indicative of the concrete and electrolyte between the reference and the bar specimen (working electrode). Impedance response at 1 Hz may capture a small part but not all of the coating and corrosion impedance in addition to the electrolyte resistance. At 1 mHz, impedance values are more indicative of the cumulative effects of the concrete and the impedance induced by both the coating, if present, the passive oxide layer on the reinforcement, and the corrosion process.

Typical Impedance Plots

The potential, impedance and phase angle data from each EIS test across the chosen frequency spectrum could be plotted in several formats to reveal information about the system and its corrosion state. The first is a Bode plot, with the modulus of impedance and the phase angle plotted as a function of the frequency of the alternating current. The second is the Nyquist plot, which presents real and imaginary components of the complex impedance response. Each of the plots is useful for determining aspects of the system, including indications of corrosion state, coating saturation, and concrete resistivity.

Interpretation of electrochemical impedance spectroscopy results is difficult for any but the simplest experimental designs conducted under tightly controlled laboratory conditions. In simple solution, a good quality coating on a metallic substrate can be clearly characterized (Standish, J. V. & Leidheiser, Jr. H., 1981; Scantlebury, J. D. & Sussex, G. A. M., 1981). However, the concrete medium as an electrolyte introduces a host of complexities regarding current distribution, interface impedances, and alternate physical and chemical interactions. Further, partially or fully disbanded coatings with moisture between the coating and the substrate add more complexity to the system. Once corrosion has initiated, the accumulation of corrosion product will provide new barriers for ion and electron flow, making the system even more complex.

The frequency range used in this study is insufficient to completely capture aspects of the electrolyte and polarization resistance related to corrosion, even for bare steel. For example, to determine precisely the electrolyte resistance would require frequency of 10 kHz or greater, which is beyond the capacity of the system employed. Polarization resistance time constants are often represented by large arc-shaped response of high real impedance on the Nyquist plot. As can be seen from Figure 11, for bare steel, arc-shaped curves are suggested at high values of real impedance, but the frequency range (high real impedance typically corresponds with low frequency on the Nyquist plot) is insufficient to fully describe the curve. Attempts to extrapolate from the available data would induce considerable error in the resulting estimates. Therefore, it

is not reasonable to determine precise polarization resistance values from the available data. However, this condition does not preclude the use of these data in determining the time of corrosion initiation.

Figure 11 presents both Bode and Nyquist diagrams of the available impedance spectrum for a typical bare steel specimen at selected times prior to (top) and after (bottom) the initiation of corrosion. The slope of the Nyquist plot (top-right) implies a very large polarization resistance, consistent with a well-developed passive layer (Sagüés, A. A. & Zayed, A. M., 1991). Considering the modulus of impedance, as shown in the Bode plots (left), as well as the magnitude of real and imaginary impedance components in the Nyquist plots (right), a clear decrease in impedance (note the difference in scales), especially at low frequencies, can be observed as corrosion occurs.

The same trends can be observed for a typical ECR specimen, as shown in Figure 12. The Nyquist plots for the ECR specimen before (top) and after (bottom) corrosion initiated correlate well with observations by Sagüés and Zayed of partially disbanded coatings in concrete (Sagüés, A. A. & Zayed, A. M., 1991). The impedance in the complex plane prior to corrosion (top-right) resembles either a system under diffusion control, or more likely, a transmission line configuration, where moisture exists beneath the coating. Again, as corrosion occurs (bottom), the low frequency impedance decreases dramatically. The magnitude of the phase angle also decreases, but also becomes more complex, as additional phenomena occur related to corrosion and coating deterioration.

Determining Corrosion Initiation

For uncoated bars, active corrosion appeared to correspond to potential values more negative than -350 mV CSE, as outlined in ASTM C 876 (ASTM, 1991). For coated bars, a similar change in electrical potential was generally observed. However, active corrosion could not be assumed unless a corresponding decrease in impedance was observed. The value of impedance at 1 mHz was determined for ECR, recognizing that the coating has a strong influence on the impedance values, and the observed behavior would be a combination of coating and corrosion related impedance factors. However, the reduction of low frequency impedance were complimented by changes in open-circuit potential, and together reliably indicate the occurrence of corrosion in the specimens. This is consistent with observations by others of ECR systems involving disbanded or partially disbanded coating (Sagüés, A. A. & Zayed, A. M., 1991).

In general, non-corroding ECR specimens exhibited a modulus of impedance at 1 mHz on the order of 10^6 ohms. A few specimens had impedances as high as 10^8 ohms, and correspondingly noble potential values, usually more positive than -200 mV CSE. Actively corroding ECR specimens had a corresponding modulus of impedance less than 10^5 ohms, and often less than 10^4 ohms.

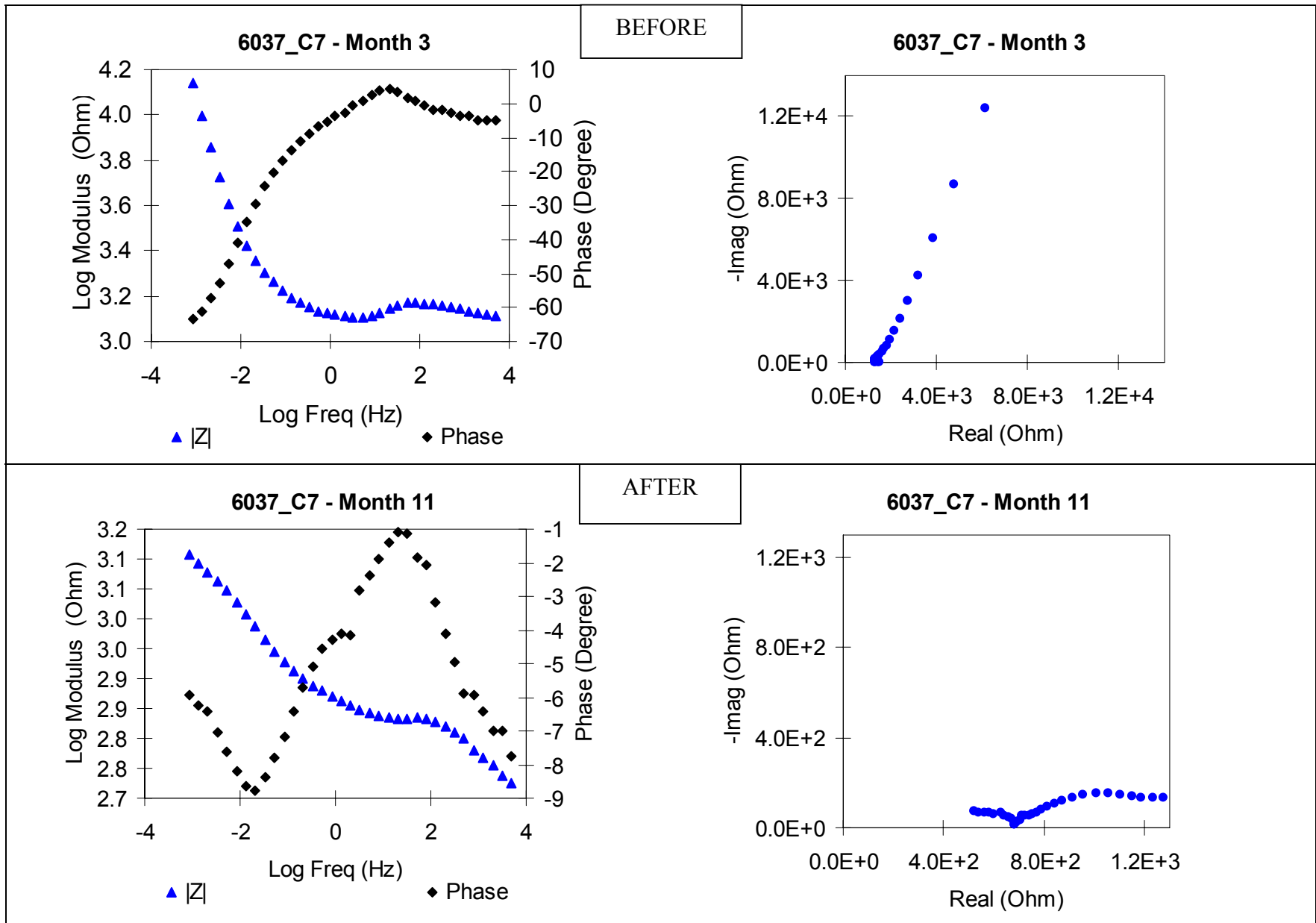


Figure 11 Typical Bode and Nyquist Plots for Bare Steel Before and After Initiation

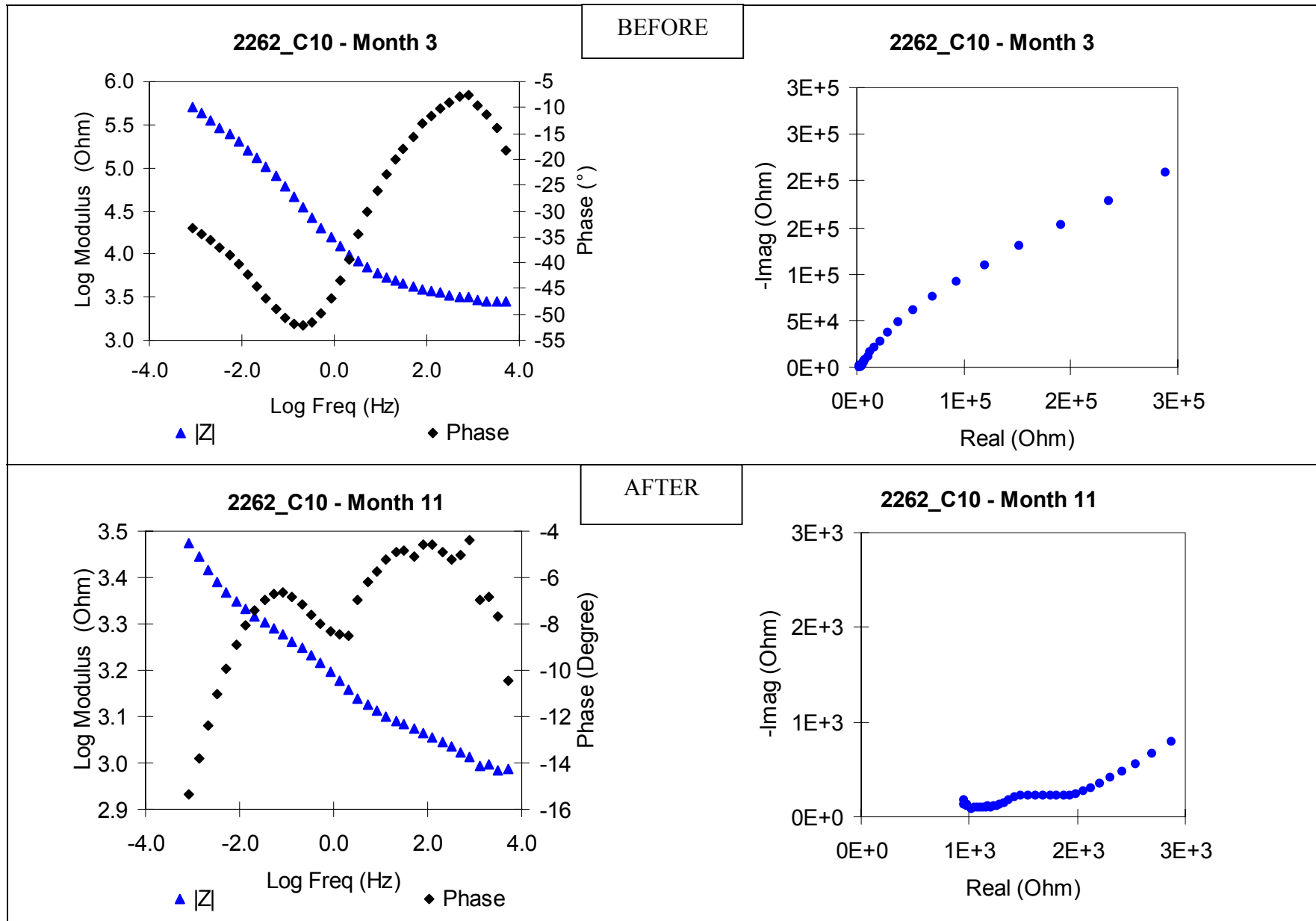


Figure 12 Typical Bode and Nyquist Plots for ECR Before and After Initiation

By observing the trends of open-circuit potential with time, changes in the system could be identified by the occurrence of sudden changes in slope or magnitude. Correlating changes in potential with shifts in impedance and phase allowed a reasonable estimation of the time of corrosion initiation, to the nearest month, which was the interval between measurements. Figure 13 presents a typical group of graphs for an ECR steel specimen that convey the trends of potential and impedance and phase angle at a scan frequency of 1 mHz. For this specimen, corrosion appeared to initiate in the sixth month of treatment.

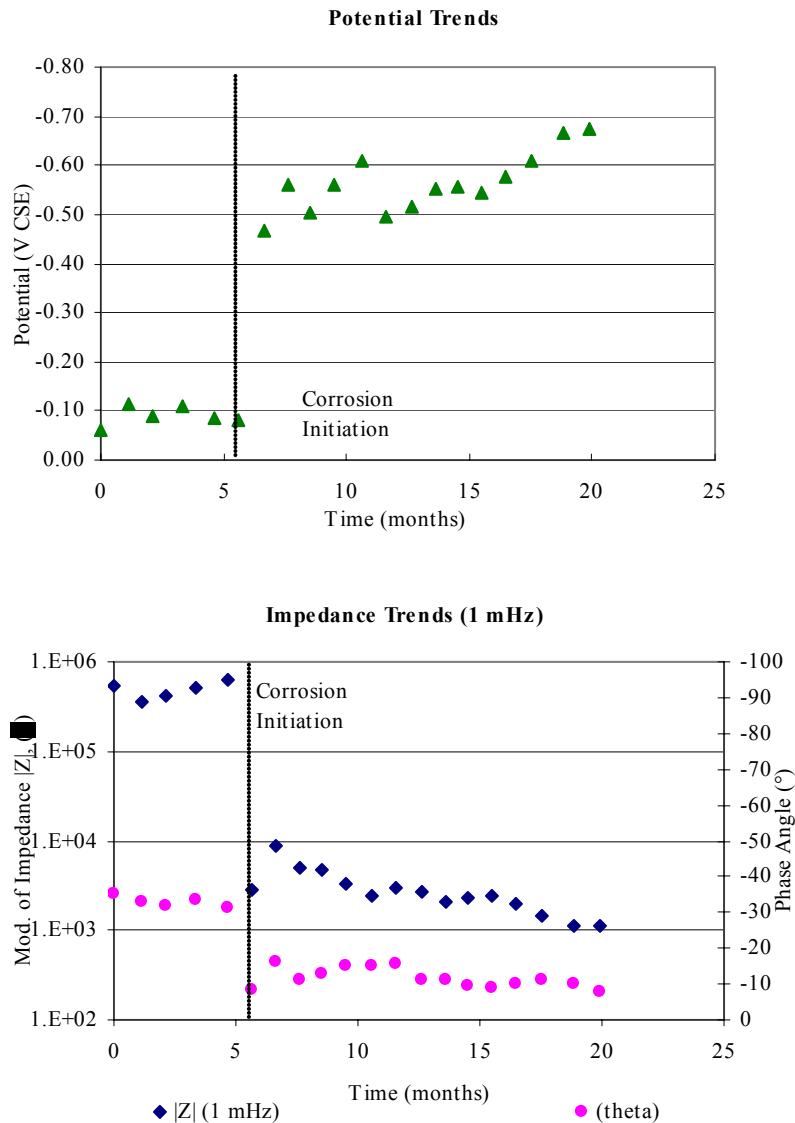


Figure 13 Potential and Impedance Trends for an ECR Specimen (typical)

For each of the specimens, the time to corrosion initiation was determined from electrical potential trends and electrochemical impedance measurements, and the time to cracking, if applicable, was determined by visual identification of cracks on the top surface of the treated specimens. The corrosion propagation period was defined as the difference between the time to

initiation and the time to cracking. Detailed tabulation of corrosion initiation times and times to cracking are presented elsewhere (Brown, M. C., 2002).

Chloride Concentrations at Time of Field Sampling and After Cracking

As outlined previously, acid-soluble chloride concentrations were obtained at two elevations of the cores above the section subject to laboratory treatment. After specimens had cracked, chloride concentrations in concrete samples taken directly above and adjacent to the active corrosion sites on the bars were also determined. Again, detailed tabulated chloride concentrations for the specimens are presented elsewhere (Brown, M. C., 2002). Following is a discussion of the findings.

DISCUSSION

Crack Frequency and Influence on Durability

Bridge deck cracks other than those associated with constituent material, physical-chemical actions and construction practices manifest themselves as linear cracks. Early-life pattern or map cracks, such as result from plastic shrinkage, do not fall within this category, and may generally be prevented with appropriate attention at the time of construction. Linear cracks may be either transverse or longitudinal relative to the direction of the traffic. Causes of linear cracking include individual or synergistic mechanisms of material subsidence, drying shrinkage, thermal expansion or contraction, and bending conditions.

The influence of cracks on corrosion service life is presently controversial (Manning, D. G., 1981; Beeby, A. W., 1978). One viewpoint is that cracks reduce service life and the other is that cracks may accelerate the onset of localized corrosion but have little influence on overall service life of a deck. The difference in viewpoint is related to the width, intensity, and orientation of the cracks (parallel or perpendicular to the reinforcing bar). Cracks parallel and directly above the reinforcing steel have much greater influence than cracks perpendicular to the bar (Beeby, A. W., 1978). With respect to crack width, it has been shown that cracks of width less than 0.3 mm have little influence on corrosion (Atimay, E. & Ferguson, P. M., 1974). However, others have shown that surface crack width has no influence on corrosion (Tremper, B., 1947; Martin, H. & Schiessl, P., 1962; Raphael, M. & Shalon, R., 1971).

The controversy over the influence of crack width on the field performance of structures exposed to chlorides may be related to the environmental exposure conditions. For coastal structures, the reinforced concrete components are continuously exposed to wetting and drying cycles of chloride-laden water. Whereas, for bridge decks in deicing salts environments, the deck is exposed to periodic cycles of chloride-laden water only during the winter months. The remaining months the deck is exposed to periodic wetting and drying cycles of rain and condensates. If chloride ions are carried into cracks during the winter months, they can also be removed during the spring-summer-fall months. This mechanism for reduction of chloride ion concentration has been clearly demonstrated in uncracked bridge deck concrete (Schiessl, P. & Raupach, M., 1997).

Equally controversial is the role of ECR in cracked concrete bridge deck sections. It has been stated that in cracked concrete sections "the reinforcing steel itself is the last line of defense

against corrosion, and the use of a barrier system on the reinforcing steel, such as epoxy coating, another organic coatings, or metallic coatings, is more critical" (Smith, J. L. & Virmani, Y. P., 2000). However, no evidence is provided as to how effective ECR is in cracked sections. Others have shown that ECR for corrosion protection was least effective in cracked sections and in relatively high permeable bridge deck concrete (Fanous, F. S. et al., 2000; Weyers, R. E. et al., 1997).

Field Crack Frequency

Table 5 presents the crack frequency for the longitudinal and transverse/diagonal cracks less than and equal to 0.30 mm and greater than 0.30 mm. As shown, the crack frequency was significantly less for the transverse cracks than the longitudinal cracks, 0.283 and 0.049 and 0.049 and 0.003, respectively for cracks less than and equal to 0.30 mm and greater than 0.30 mm. The crack frequency of the BS decks appears to be less than the crack frequency of the ECR decks. The average crack frequency for the 10 decks in this study was found to be 0.383 linear meters of crack per square meter of deck.

Crack Width and Depth in Cores

Various forms of regression fit, including linear, polynomial and logarithmic equations, were used to try to describe a relation between crack width and crack depth. Figure 14 presents a second-order polynomial model that best fit the data for core crack depth as a function of core crack width. As shown, there is not a strong correlation between crack width and depth. The correlation coefficient, R^2 , was only 0.403. Also, no correlation could be found between crack surface width and age or crack depth and age. Thus, a visible surface crack does not, in most cases, extend to the depth of the reinforcing steel. Also, a wider surface crack does not necessarily mean the crack is deeper.

Table 5 Bridge Crack Frequency

Survey Age (years)	Crack Frequency (m/m ²)			
	Crack Width ≤ 0.30 mm		Crack Width > 0.30 mm	
	Longitudinal	Transverse	Longitudinal	Transverse
4	0.201	0.123	0.017	0.014
6	0.394	0.208	0.008	0.000
7	0.301	0.123	0.000	0.004
9	0.475	0.065	0.084	0.003
12	0.072	0.000	0.072	0.000
14	0.735	0.000	0.015	0.000
15*	0.079	0.038	0.044	0.006
16*	0.000	0.000	0.000	0.000
16	0.416	0.000	0.111	0.000
18	0.179	0.000	0.088	0.000
Sample Frequency	0.283	0.049	0.049	0.003

* Designates decks containing bare steel. Remaining decks were constructed with ECR.

Frequency of Cracks ≤ 0.30 mm wide	0.331 m/m ²
Frequency of Cracks > 0.30 mm wide	0.051 m/m ²
Cumulative Sample Crack Frequency	0.383 m/m ²

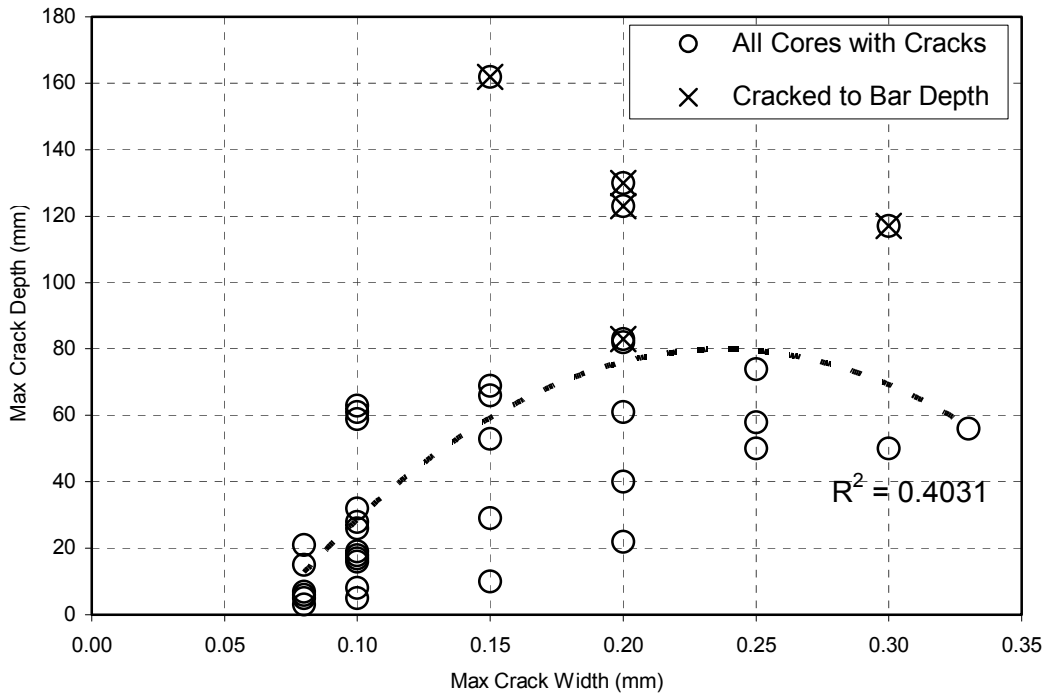


Figure 14. Crack Width and Depth

Chloride Concentration at Cracks and in Uncracked Locations

Average chloride concentration penetrating to depths of about 13 mm below the surface and about 19 mm above the bar depth were measured and plotted as a function of age, as shown in Figure 15 and Figure 16, respectively. However, note that background chloride content of samples of the same concrete mixture typically varies by 0.2 kg/m³ (Brown, M. C. et al., 2001). Thus, chloride contents in a crack sample would have to be more than 0.2 kg/m³ greater than the chloride content adjacent to the crack to clearly indicate a significant increase in chloride due to the crack.

While investigating the influence of cracks, the relation to surface width of chloride content at 13 mm below the surface and 19 mm above the bar resulted in poor correlation coefficients of R² = 0.18 and R² = 0.10 for the best-fit models, respectively. When considering the influence of crack depth, the strongest correlation for chloride concentration at 13 mm below the surface was a polynomial curve, with an R² = 0.20, still a poor indicator. For the relation of chloride concentration to crack depth at 19 mm above the bar, the best correlation coefficient was only R² = 0.14. Thus, chloride concentration at cracks could not be predicted by crack width or crack depth.

In the following discussion, chloride within cracks are compared to uncracked concrete and plotted according to the age of each bridge deck. Note that the chloride contents are not solely a function of age, but may also be a function of route type and location, since driving surface chloride concentration, C_o, varies according to these environmental factors. Figure 15 presents the chloride concentrations at a depth of 13 mm at individual cracks versus the 95%

confidence interval of chloride concentrations derived from the sample distributions of cores from uncracked locations on the same decks. Ten chloride contents were within the 95% confidence limits (CL), 8 were less than the 95% lower limit (LL) and 10 were greater than the 95% upper limit (UL). Also, the average increase for those values exceeding the 95% upper confidence limits was small, approximately 18.6%. There appears to be no significant difference between chloride contents at cracks and uncracked sections at a depth of 13 mm, but the variability between individual locations seems to be higher.

Figure 16 presents a comparison between individual chloride contents at cracks and the 95% confidence limits of uncracked core sections at a depth of 19 mm above the reinforcing bar. Of the 18 chloride contents at 19 mm above the bar at cracks, 7 were within the CL and 11 were above the 95% UL. Thus, it appears that cracks influence the chloride content at a depth 19 mm above the reinforcement 61% of the time. In these instances, the average increase in chloride concentration appeared to be about 0.6 kg per cubic meter of concrete beyond the 95% UL. As is clear from Figure 16, all of the instances of increased chloride concentration at this depth were observed in decks less than 10 years of age, whereas decks greater than 10 years of age showed no significant difference in chloride concentration relative to cracks. The lack of influence of cracks on chloride penetration at later ages may be related to autogenous healing and/or carbonation products. Such reactions may result in the accumulation of products that serve to fill the crack and impede chloride ingress.

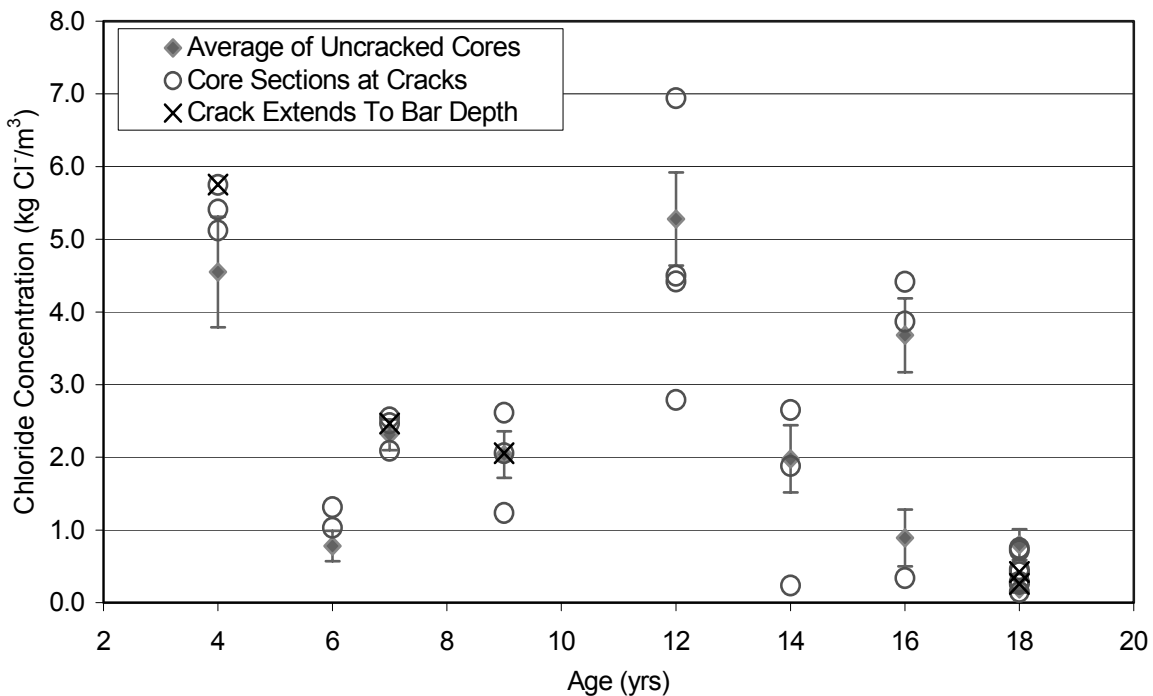


Figure 15 Comparisons of Chloride Concentration at 13mm below Surface

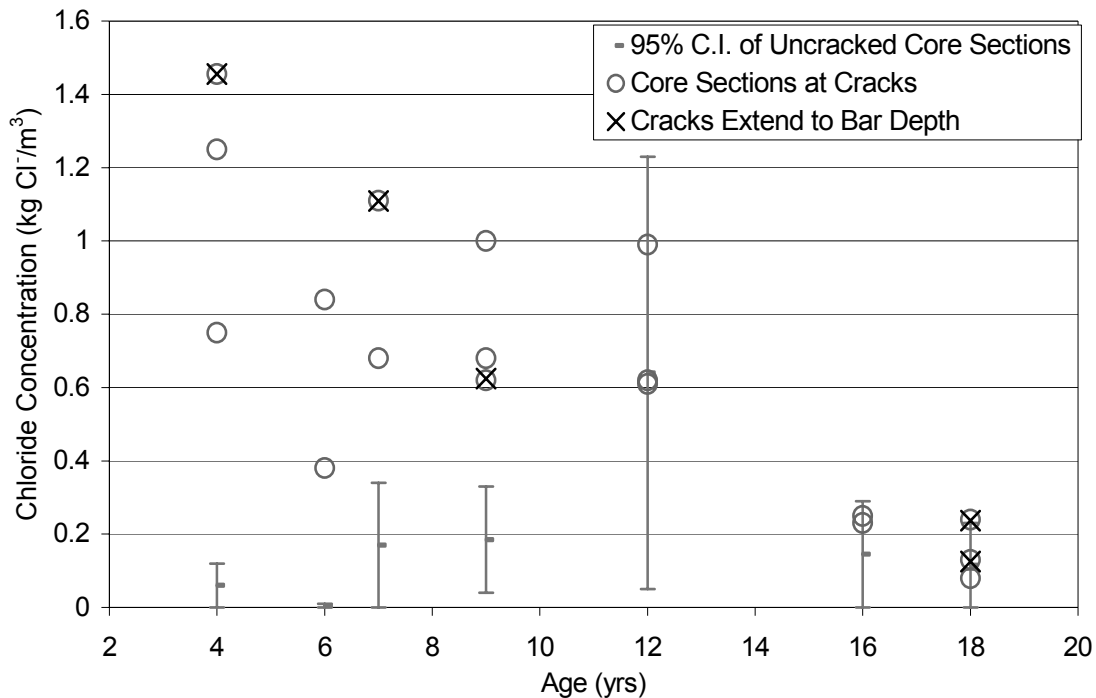


Figure 16 Comparisons of Chloride Concentration at 19mm above the Bar

It is important to consider the overall impact of increased chloride penetration. If increased chloride from a crack centered above and parallel to the reinforcement induces corrosion and spalling, it could be reasoned that the spall-related cracks from that bar radiate to the surface at approximately a 45° angle on either side of the bar. If the average clear cover depth over the bar were 65 mm, as observed in this study, then the tributary width of the spall along the crack would be approximately 130 mm.

Some consider the crack corrosion influence zone to be 3 times the bar diameter or in this case about 100 mm wide (Babaei, K. & Hawkins, N. M., 1988; Lorentz, T. & French, C., 1995). However, this generally pertains to influence along the length of a bar, from a transversely intersecting crack, and does not likely apply to diffusion about a bar into non-fractured cement paste regions.

Nonetheless, as a worst-case, consider for a total crack frequency of 0.383 m/m² (Table 5) and a corrosion influence zone 130 mm wide, that all 61 percent of the cracks where the chloride content at the crack is greater than uncracked sections are located in a single span lane. The resulting deck area affected by this cracking is projected to be 3.0 percent. Twelve and one-half percent damage in the worst span-lane is considered the rehabilitation damage level (Fitch, M. G. et al., 1995). Thus, the cracking frequency of the worst span-lane would have to be about 5 times the cracking frequency measured in this study to influence the time to rehabilitation. Further, 2.5% to 3.0% damage may be associated with the level of deterioration at the time of first repair. Therefore, damage induced by linear cracking, may accelerate the onset of the first repair activities, but once addressed, is unlikely to significantly shorten the bridge deck service life.

Accelerated Laboratory Treatment and Monitoring

Laboratory treatment and monitoring were undertaken to assess the relative times to corrosion initiation, times to cracking, and associated chloride concentrations at the reinforcement for both bare steel and ECR. Comparisons were then made to determine what expected service life benefit is attributable to the use of ECR. Table 6 presents a summary of the disposition of core samples after 36 months of treatment.

Table 6 Summary of Sample Status

Core Classification		Subtotal
Remaining Cores	Initiated Corrosion	28
	Corrosion Not Initiated	13
Terminated Cores	Cracked (ECR)	25
	Cracked (Bare Steel)	28
	Truncated (Corrosion Initiated)	24
	Truncated (Corrosion Not Initiated)	23
Total		141

Time to Corrosion Initiation and Cracking

Table 7 presents the average time from first application of the ponding treatment required to initiate corrosion, the time until cracking was observed, and the propagation time which passed between those benchmarks. The information is summarized for bare steel and for ECR specimens for which observations are available after 36 months of treatment. Note that corrosion initiated for a significant number of specimens in the ECR group that have not yet reached cracking. Hence, the average propagation time does not necessarily correspond to the difference between average time to initiation and average time to cracking.

Table 7 Average Times to Initiation and Cracking for Bare Steel and ECR

		Time to Initiation [†] (yrs)	Time to Cracking (yrs)	Propagation Time (yrs)
Bare Steel	Average	0.20	1.21	1.01
	StDev	0.19	0.49	0.46
	CoV (%)	98%	40%	46%
	n	28	28	28
ECR	Average	0.89 (0.91)	1.75	1.42
	StDev	0.79 (0.81)	0.49	0.57
	CoV (%)	89% (89%)	28%	40%
	n	77 (69)	25	25

[†] Primary values represent the sample set of 113 ECR cores. Values in () were taken from a subset of 96 specimens, which excludes 17 ECR specimens for which treatment was truncated after 22 months.

To visualize the relative rates of corrosion initiation, the cumulative probability of initiation of bare steel versus ECR has been plotted in Figure 17. Note that the number of points for each distribution does not match the total number of observations for each bar type, since observed corrosion initiation might occur for more than one sample at a time, and therefore overlap. Although the chloride concentrations at bar depth prior to ponding treatment were predicted to be very low for most specimens, more than 50% of the bare steel specimens initiated corrosion within the first two months of treatment. Although the sample size was greater, it took approximately 1.2 years for a corresponding percentage of the ECR bars to initiate corrosion. These observations will be discussed further in the chloride diffusion rates and concentrations sections.

Since the time to corrosion initiation depends upon the arrival of chlorides at the steel surface, and some period of exposure is necessary to depassivate the steel, it was not deemed appropriate to make final judgments based upon a direct comparison of time-to-initiation for the two groups. Variations in diffusion rates and surface concentrations between different decks, comprised of different concrete mixtures, even under the same specification, would significantly impact the initiation of corrosion.

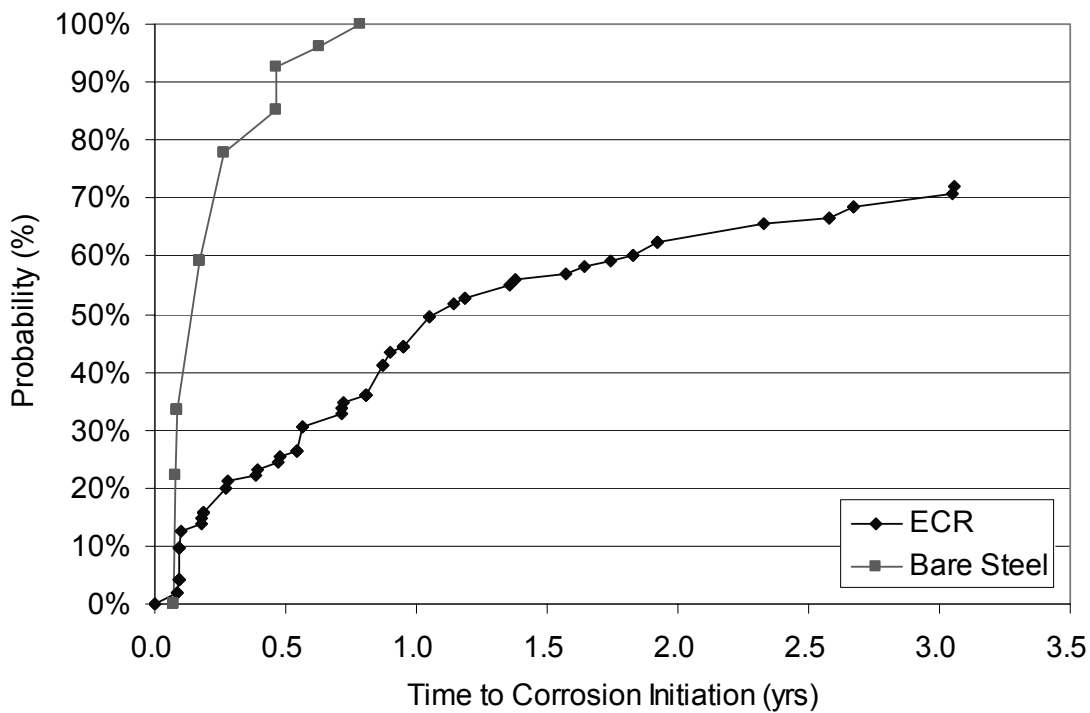


Figure 17 Comparison of Time to Initiation under Laboratory Exposure

Figure 18 presents the cumulative probability for the time to cracking for the bare steel and the ECR groups. Again, time to cracking was the same for some specimens, resulting in overlapping data points. Over the 36 month treatment period approximately 26% of the ECR specimens cracked (excluding the specimens truncated at 22 months), compared to 100% of the bare steel specimens. At the beginning of observed cracking, difference in time-to-cracking was only about 0.5 years, but gradually increased to an almost 2 year difference after 36 months

exposure. Comparing the 12th percentile of the groups shows an increase in time to cracking of approximately 1 year for the ECR, as compared to the bare steel. Time-to-cracking results for ECR observed are significantly less than in previous laboratory studies that compared new bare steel and ECR specimens, where the epoxy coating was well bonded to the steel substrate (Clear, K. C., 1992).

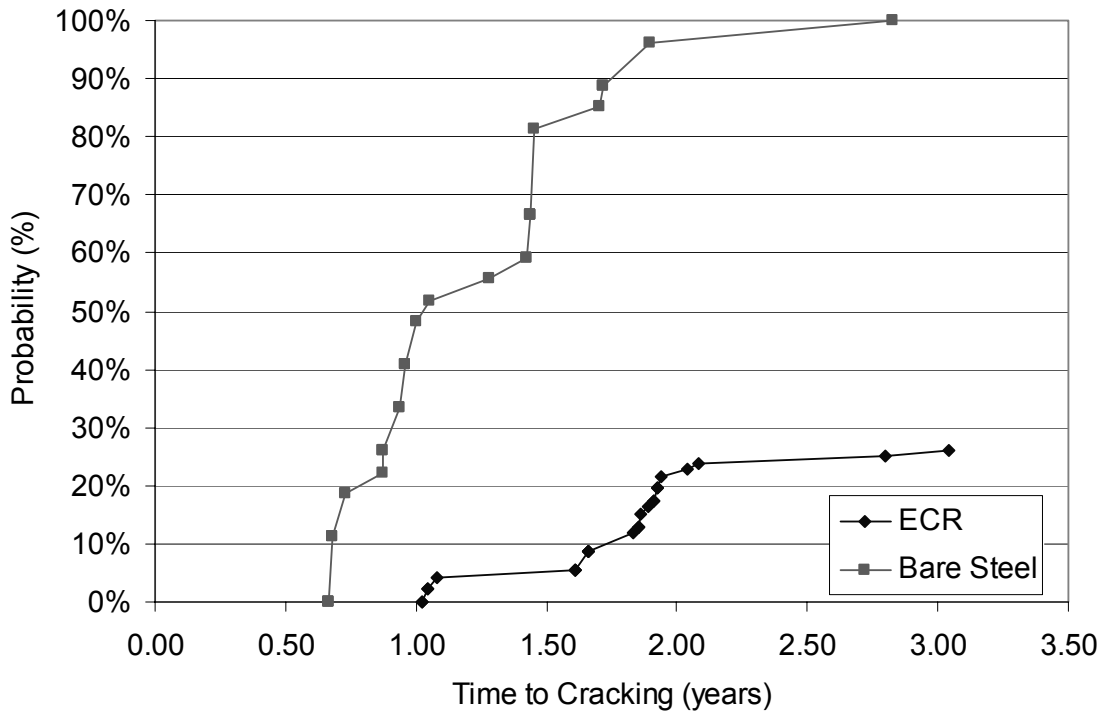


Figure 18 Comparison of Time to Cracking under Laboratory Exposure

Propagation Time

Subtracting the time-to-initiation from time-to-cracking gives the active corrosion propagation time, during which corrosion products accumulate, pressure develops, and finally the cover concrete fractures. Figure 19 presents histograms of the observed propagation periods in laboratory testing for both bare and epoxy-coated reinforcement. The average propagation time for bare steel was 1.01 years in this study, and the average propagation time the ECR specimens cracked to date was 1.42 yrs.

It might be argued that the rate of corrosion could be influenced both by the rate at which chloride concentration increases at the bar, and by the resistivity of the concrete between anode and cathode sites on the steel. Under the accelerated test conditions, it is possible that the corrosion rate in some or all of the specimens is cathodically limited by the availability of oxygen at the cathode(s), which is also a function of the concrete diffusivity and degree of saturation. Since corrosion anode and cathode reactions must be balanced, a "starved" cathode will slow the anodic reaction. However, the mechanism of corrosion underneath a disbanded coating becomes altogether different, and no longer depends upon the diffusion of oxygen to the cathode. The confined electrolyte beneath the coating becomes more acidic, promoting the corrosion reaction.

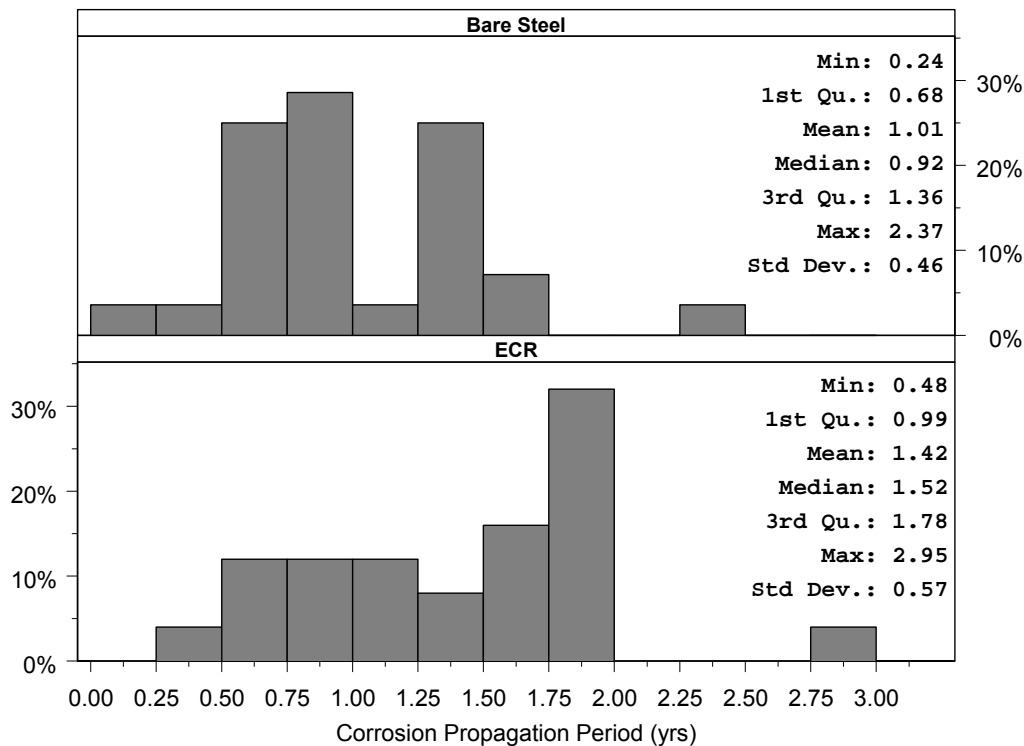


Figure 19 Histograms of Corrosion Propagation Period for BS and ECR

The specimens in this study were taken from locations directly adjacent to those of a preceding study, usually within 0.5 m, and along the same bar. Thus, the condition of the coating was assumed to be similar at the time of sampling to that of the companion specimens from the previous study. An attempt was made to correlate the observed time-to-cracking with available data that may be used as predictors of performance. The coating parameters considered were holidays, percent surface damage, and thickness, all of which were taken from observations in the previous study, in which the bars were extracted from the deck and directly observed for various parameters (Pyc, W., 1998). Concrete parameters included the moisture absorption capacity, degree of saturation, effective field diffusion coefficients, and clear cover depth of the original core obtained in this study.

For bare steel, the strongest correlation to time-to-cracking was the degree of saturation of the concrete prior to ponding. A higher initial degree of saturation corresponded to a greater time to cracking. The correlation, however, was very weak ($R^2 = 0.053$), and would be a poor predictor of performance. For ECR, time-to-cracking could be best modeled as a function of the percent of damaged surface area of the coating, as mashes, dents, or scrapes, and the effective rate of diffusion estimated from the core chloride data at 13 mm below the surface and 19 mm above the bar. The correlation coefficient, R^2 , was 0.86. Other concrete and coating parameters did not appear to improve the prediction. Although percent damage was a strong predictor, the percent damage to coatings was very low, ranging from none to 2.1%, with a mean of 0.2% among bars that did exhibit damage. The range of holes per bar was 0 to 1, with a mean of 0.04, and coating holidays ranged from 0 to 10, with a mean of 1.9, respectively, for companion specimens of ECR bars cracked to date.

Results from the previous study suggested a relation might be found between the degree of coating disbondment and the time to cracking. The regression analysis considered this possible relation, but did not find a correlation. This is likely due in part to the time that passed, two years, between field sampling in the two studies. During this time, additional adhesion loss between the coating and the steel may have occurred. In addition, the difference in physical locations of the respective specimens, even though they were from the same reinforcement bar and less than 0.5 m apart, could contribute to variability when comparing results from the two studies. Therefore, the lack of correlation of these results does not necessarily indicate that no relation exists between degree of disbondment and time to cracking.

Time to corrosion initiation and cracking were determined for accelerated laboratory exposures. Therefore, further analysis was required to predict corrosion in field structures based on the laboratory observations.

Chloride Concentration at Reinforcement Depth after Cracking

Since direct comparison of initiation and cracking times could not be directly related to field conditions, analysis was conducted on the concentrations of chloride after cracking occurred and estimates of chloride concentration at the reinforcement depth at the time of initiation.

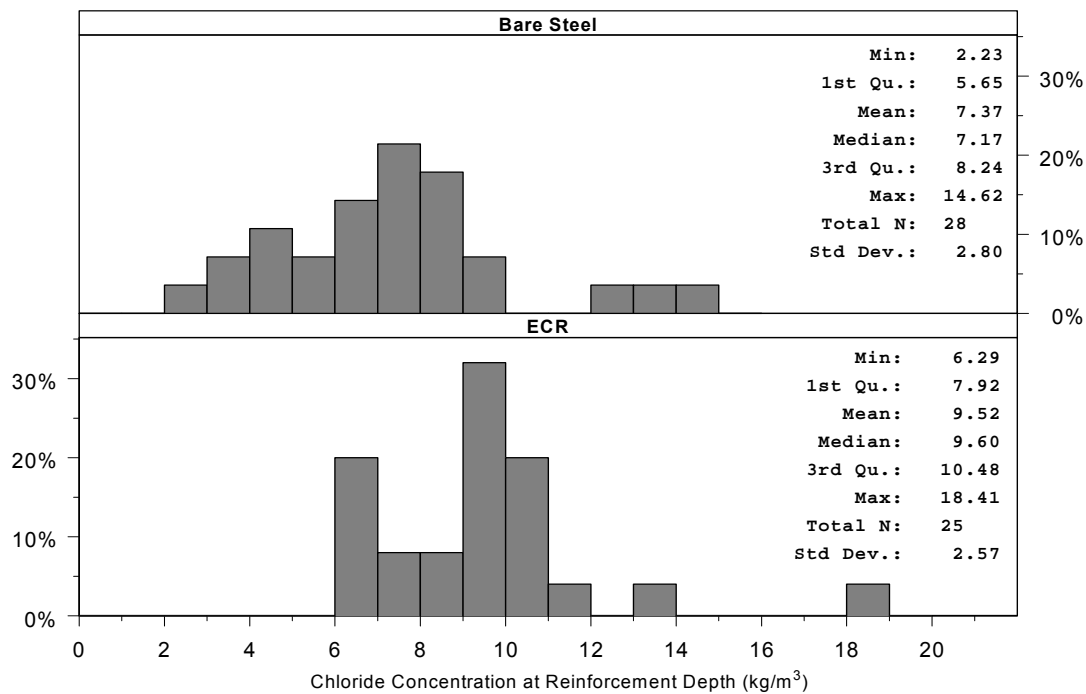


Figure 20 Chloride Concentration at Reinforcement Depth after Cracking

Figure 20 presents histograms of the chloride concentration at the steel depth at the time of cracking, as an average of concentrations measured in concrete immediately to the left and the right of the actively corroding section of the reinforcement. Concentrations were expressed on the basis of weight per unit volume of concrete, assuming a nominal concrete density of

2,323 kg/m³, and reduced by the nominal background chloride concentration for each bridge to reflect "diffused" chloride. The distributions of chloride concentration for bare steel and ECR were each approximately normal in shape. The average concentration for the two chloride contents at the active corrosion site for bare steel ranged from 2.23 kg/m³ to 14.62 kg/m³, with a group average concentration of 7.37 kg/m³. For ECR, the concentrations ranged from 5.25 to 18.41 kg/m³, with a group average chloride concentration of 9.52 kg/m³.

Using a direct sampling method, a quick simulation was run to determine the approximate range and distribution of differences between chloride concentrations after cracking for ECR and bare steel. By selecting at random an observed chloride concentration at the reinforcement depth after cracking for ECR, and subtracting from it an observed chloride concentration after cracking for bare steel, also selected at random, an approximate ΔCl_{cr} was determined. Repetition of this operation for 10,000 iterations revealed an approximate distribution for ΔCl_{cr} , as shown in Figure 21. Thus, based on the observed laboratory chloride concentrations, ECR required an average of 2.35 kg/m³ more chloride than bare steel to induce cracking. This may be influenced by both the corrosion initiation and the propagation phases of the deterioration process. However, 95% confidence intervals for this estimated ΔCl_{cr} ranged from -4.04 to 8.75 kg/m³. Therefore, there is no guarantee that ECR will outlast bare steel in all cases. Since these values were from accelerated laboratory tests, during which diffusion rates appeared to be an order of magnitude greater than those observed for field concrete, further analysis was warranted.

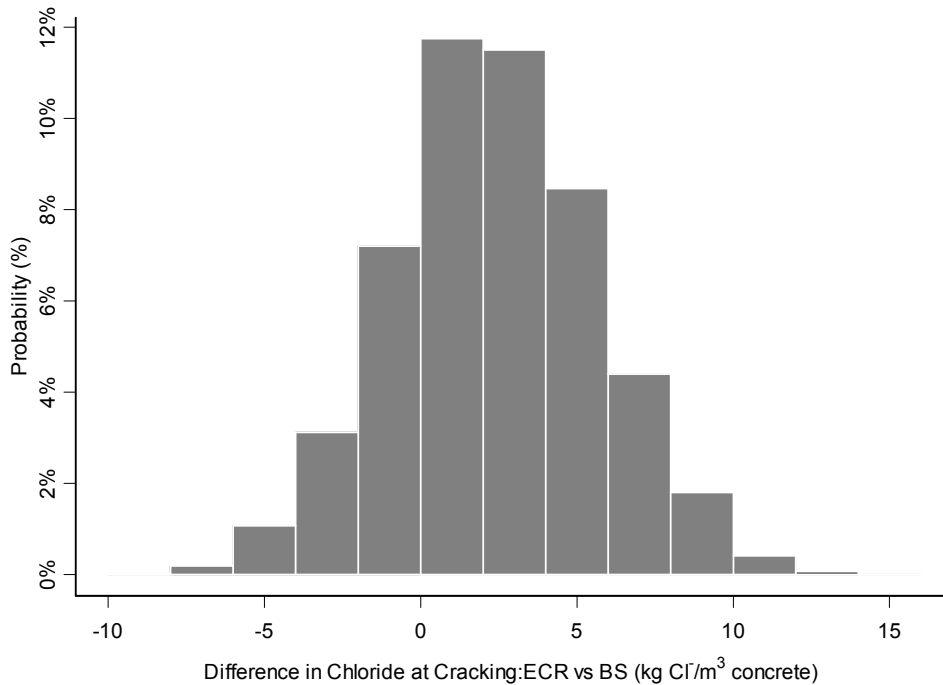


Figure 21 Chloride Concentration Difference: ECR minus Bare Steel (ΔCl_{cr}) under Laboratory Treatment

Estimating Chloride Concentration at Reinforcement Depth at Corrosion Initiation

Using the age of the structures at the time of sampling, initial chloride concentration measurements at 13 mm from the deck surface and at 19 mm above the reinforcing steel, and the measured clear cover depths of the reinforcing bars, the effective diffusion rate of chloride under field exposure was approximated. Next, the computed chloride profile for each core was used to approximate the concentration of diffused chloride at the reinforcing steel depth. Most of the specimens were projected to have chloride concentrations no greater than background levels.

Bar influence

Recent literature has also brought to light the potential for significant influence by the bar on chloride accumulation at the leading face of the reinforcing steel (Kranc, S. C. et al., 2002). The presence of the rebar acts as a local barrier to diffusion within the concrete matrix. The authors stress that the presence of the bar can significantly increase the rate of chloride concentration increase at the leading face of the bar, leading to overestimations of the time to corrosion initiation. The effect becomes more severe as the ratio of bar diameter to clear cover increases, but reaches a limiting value, dependent upon the ratio of surface concentration to the initiation concentration at the bar. A de-rating factor was proposed, dependent upon ratios of bar diameter to clear cover, and surface concentration to threshold initiation concentration.

However, if chloride concentration is determined from samples obtained directly adjacent to the reinforcement, the authors speculate the resulting effective diffusion rate may inherently address the effect of the rebar as a barrier. Chloride concentrations for this case were determined immediately adjacent to the steel, and the increased rate of chloride accumulation at the bar is assumed to be inherently addressed within the apparent diffusion coefficient. Since the clear cover and nominal bar diameter, and chloride treatment was approximately the same for all specimens, any actual influence should not greatly affect direct comparisons of the study groups.

Capillarity

For the treatment phase of this study, it is noted that the cores were at a relatively low saturation level when ponding initiated. Capillary action is expected to have had a significant influence on chloride uptake during the initial ponding. However, once saturated, the specimens were likely to have reverted to behavior more closely resembling diffusion-controlled chloride migration.

Therefore, the ingress of chloride through the concrete cover to the reinforcing steel depth during the cyclic ponding treatment was also modeled using the same one-dimensional solution to Fick's Second Law of Diffusion. After cracking and chloride evaluation at and above bar depth of the treatment cores, the rate of diffusion and approximate driving chloride concentration were calculated, where possible. The resulting pseudo-diffusion coefficients were generally an order of magnitude greater than the effective diffusion coefficients calculated for field exposures, and C_0 concentrations were generally between 10 kg/m^3 and 20 kg/m^3 .

To better understand the potential distribution of chloride within the pore system, it was useful to know whether it is possible for such concentrations to be contained entirely within the pore solution, or if some level of chloride binding or other physical phenomena was required.

The authors investigated the saturation limit of chloride in a simulated concrete pore solution (Diamond, S., 1981). The saturation concentration of NaCl in pure water is approximately 360 g/L. The average of three simple laboratory trials revealed a saturation concentration of NaCl in simulated pore solution of approximately 339 g/L, or 15.2% Cl⁻. The average absorption of concrete in this study was 5.76 percent by weight. For normal weight concrete (2322 kg/m³), the pore solution could then be estimated to account for 130 kg/m³. The resulting saturation concentration of Cl⁻ in concrete pore solution is estimated to be 20 kg/m³ (33 lb/yd³). Thus, the chloride represented in the observed C_O concentrations could be contained entirely within the pore solution under saturated condition.

Using the pseudo-diffusion rates and surface chloride concentrations, in conjunction with the observed propagation period, the amount of chloride that would have diffused during active corrosion was calculated, again using a one-dimensional solution of Fick's Second Law of Diffusion. Subtracting the estimate of chloride diffused during active corrosion from the total chloride present after cracking resulted in an approximation of the chloride present at bar depth at the time of corrosion initiation.

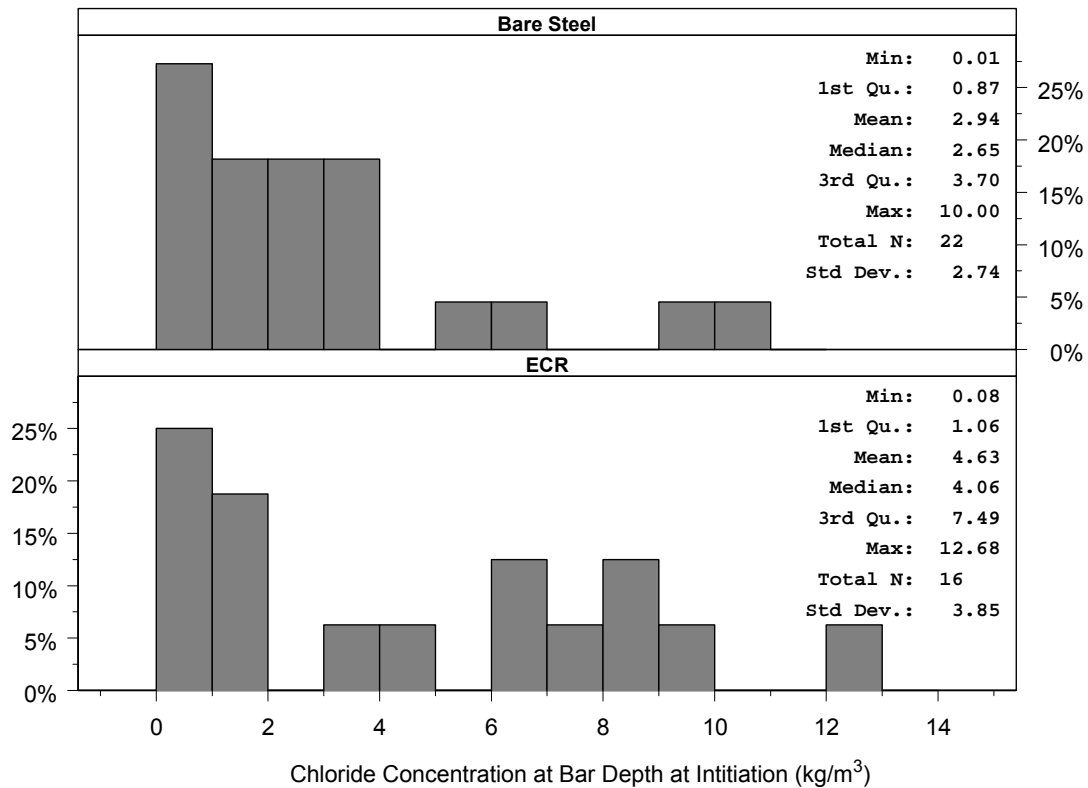


Figure 22 Estimate of Chloride Concentration at Reinforcement Depth at Corrosion Initiation

Figure 22 compares histograms of the estimated chloride at initiation for ECR and bare steel in cores that have cracked to date. The range of estimated chloride initiation levels for bare steel was 0.01 kg/m³ to 10.00 kg/m³, with an average of 2.94 kg/m³ and standard deviation of 2.74 kg/m³. These values are in reasonable agreement with other reports of chloride initiation under field exposure, which ranged from 0.59 to 8.75 kg/m³ (Glass, G. K. & Buenfeld, N. R., 1997; Stratfull, R. F. et al., 1975; Vassie, P., 1984; Matsushima, M. et al., 1998).

The estimated initiation range for ECR was broader, and appears to be bimodal. The range was 0.08 kg/m³ to 12.68 kg/m³, with an average of 4.63 kg/m³. However, it might be considered that the set represents two distinct groups. The group of lower initiation concentration values appears to range from 0.08 to 1.92 kg/m³, with an average of 1.03 kg/m³. The higher initiation concentrations range from 3.59 to 12.68 kg/m³, with an average concentration of 7.42 kg/m³.

Evaluation of Parameters Influencing Corrosion

As outlined previously, 17 ECR specimens were selected after 22 months for evaluation to surmise the status of the ECR specimens that had not yet cracked. Based upon impedance measurements, nine of the specimens truncated at 22 months were not believed to have initiated corrosion. The absence of corrosion was corroborated by visual observations of the bars after cutting. After 36 months of exposure, another 30 specimens, including 15 in which corrosion had initiated and 15 that had not initiated, were selected at random for evaluation.

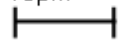
After 22 months of treatment, the cause(s) and significance of the two groups of chloride initiation concentrations were investigated by considering the direct and interactive relationships of chloride concentrations to various coating and concrete parameters. As with the time-to-cracking correlations, the coating parameters considered were holidays, percent surface damage, and thickness, all of which were taken from observations in the previous phase of study, in which the bars were extracted from the deck and directly observed for various parameters (Pyc, W., 1998). Concrete parameters included the moisture absorption capacity, degree of saturation, effective field diffusion coefficients, and clear cover depth of the original core.

The strongest correlation between bar and concrete parameters and the estimated chloride initiation concentration was the concrete saturation level prior to ponding ($R^2 = 0.56$). However, this observation was of limited use, as it was based upon only 7 observations for which both chloride initiation estimates and companion core coating and concrete data were available. What is of interest is that the percent damage to the coating or number of holidays could not be correlated within this small subset of cores, as it was with the time-to-cracking. Even so, the percent damage for the observed cores was low, ranging from none to 2.1% in one case. The average of percent damage was only 0.2%. The number of holidays per meter of bar was also low, ranging from 0 to 10, with an average of less than 2. These observations are generally within specifications applicable at the time of construction, as well as current specifications (ASTM, 2001).

After 36 months exposure, 30 additional cores were also analyzed to assess the concrete and coating parameters that correlate with corrosion of ECR. The following discussion of coating parameters pertains to a 22-specimen subset of those specimens that either cracked or were truncated during the first 22 months of treatment, as well as the 30 specimens evaluated after 36 months. At that time, additional parameters of the concrete and the coating after treatment were evaluated. These parameters included moisture content and degree of saturation of the concrete during treatment, moisture content of the coating, glass transition temperature of the coating, and the presence and degree of micro cracking in the surface of the coating.

Observation of the Coating Surface

Samples of the epoxy coating were removed from the reinforcement after the treatment period was completed. The samples were observed with a scanning electron microscope (SEM) at various magnifications to observe the condition of the outer surface of the coating. The degree of surface cracking of the epoxy coating was rated for 22 ECR samples that had cracked or been terminated after 22 months of treatment. The rating scale ranged from 1 to 4, representing surfaces that exhibited no cracking to severely cracked surfaces, respectively, as illustrated in Figure 23. The results are presented in Table 8. The average of 22 measured crack ratings was 2.16. The most frequent was a rating of 1 and the fewest specimens were rated 4. This data is presented in a histogram in Figure 24.

10 μ m


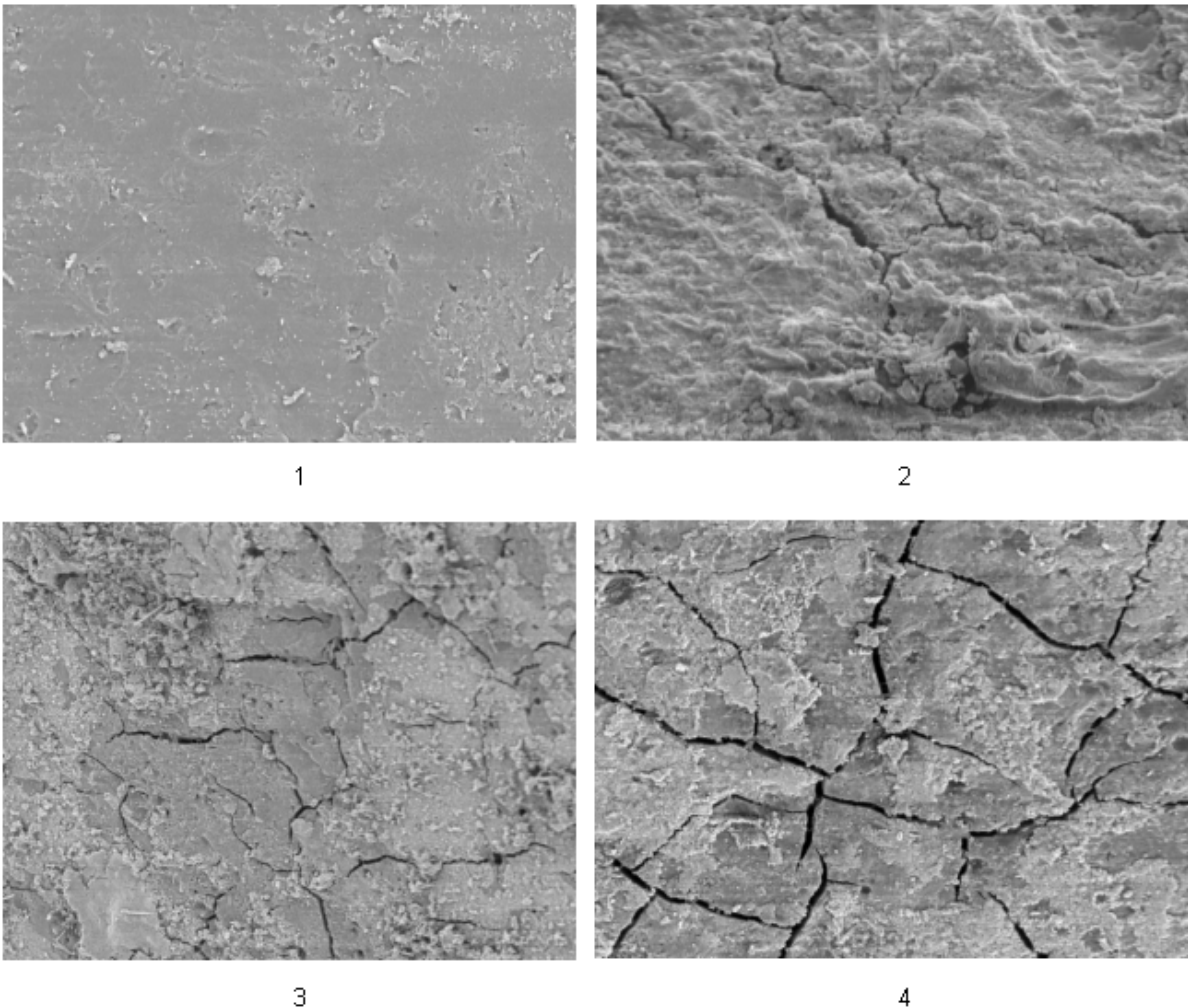


Figure 23 Visual Rating of Observed Cracks in Coating under SEM (2000 \times)

Table 8 Summary of Coating Tests for Select ECR Specimens

Bridge	Specimen	Age (yrs)	Initiation (yrs)	Propagation (yrs)	Epoxy Moisture (%)	T _g (°C)	Full T _g (°C)	Δ T _g (°C)	Crack Rating (#)
1136	C7	4	0.10	1.52	1.05	82.12	103.62	21.50	1
1136	C11*	4	0.10	-	0.39	93.99	104.09	10.10	1
1136	CR3	4	0.00	1.61	0.48	91.34	102.05	10.71	1
1004_6	C3*	6	-	-	1.14	83.85	116.54	32.69	4
1004_6	C7	6	0.09	1.78	0.60	82.27	112.36	30.09	3
1004_6	C11	6	0.55	0.48	0.42	84.85	112.92	28.07	2
1001	C2	7	0.90	0.99	0.50	102.64	112.86	10.22	1
1019	CR2*	9	0.87	-	0.84	89.17	113.25	24.08	2
1019	CR3	9	0.39	0.69	0.68	85.23	114.55	29.32	3
1015	C1	12	1.18	0.67	0.92	81.95	113.67	31.72	2
1015	C10	12	0.09	1.85	0.81	87.85	115.14	27.29	2
1015	CR3	12	0.09	1.76	1.39	70.39	114.39	44.00	1
2262	C8	14	0.18	1.48	1.03	66.80	115.73	48.93	4
2262	C10	14	0.47	1.19	0.91	68.09	115.36	47.27	4
2262	C11*	14	-	-	0.92	64.54	114.55	50.01	3
2262	CR2	14	0.10	1.81	1.17	86.23	112.93	26.70	3
1004_3	C1	16	0.18	1.75	0.33	69.45	107.86	38.41	2
1004_3	C3	16	0.81	1.12	1.27	86.35	105.98	19.63	1
1004_3	C9*	16	0.57	-	1.10	85.84	107.25	21.41	1
2021	C4*	18	-	-	0.61	84.39	97.45	13.06	1
2021	C6	18	0.09	0.96	0.61	85.04	90.90	5.86	2
2021	CR1	18	0.55	0.50	0.57	84.83	102.67	17.84	1

* Specimen treatment was truncated and bar evaluation was performed after 22 months treatment.

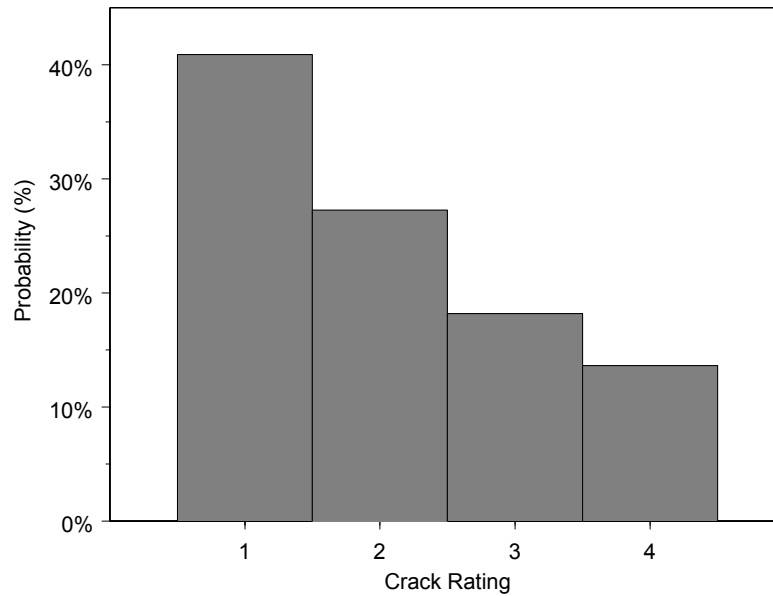


Figure 24 Histogram of Crack Ratings of Coating Surface

The crack width was also observed for some of the severely cracked ECR samples. Figure 25 shows an SEM photograph magnified at 10,000x for a specimen from the 1019 bridge. The crack width, measured at two locations, averaged 1.962 μm . The observed crack width suggests that a water molecule, approximately $9.85 \times 10^{-5} \mu\text{m}$ (0.985 \AA) in width, or even a chloride ion ($3.62 \times 10^{-4} \mu\text{m}$ diameter) could potentially enter or breach the epoxy coating, depending on the depth of the cracks. Unfortunately, it was not possible in this study to determine the depth of the observed cracks in the coating.

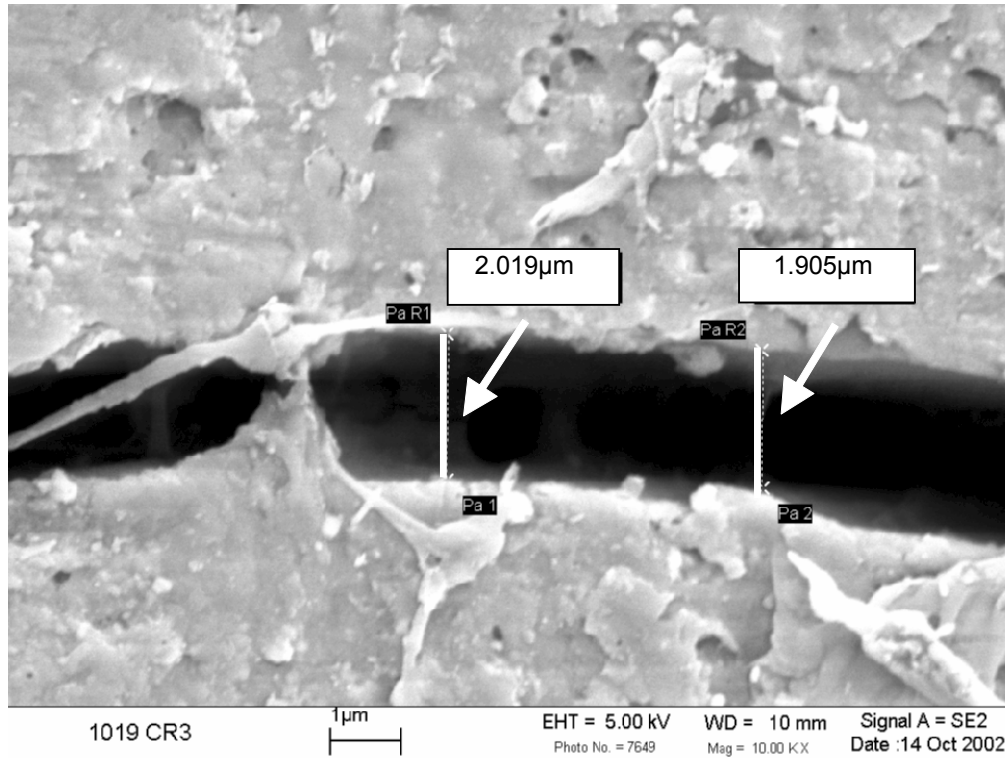


Figure 25 SEM Photomicrograph of Surface Crack in Epoxy Coating (10000x)

Epoxy Moisture Content

The moisture content for the epoxy coating was acquired using a TGA device that heats a specimen and measures weight versus temperature over time for a given sample. Moisture content is measured by the amount the weight decreases from moisture loss at elevated temperatures beyond the boiling point of water. Samples of epoxy weighing approximately 4.0g were used for the moisture content measurements. The temperature was raised to 150.00°C and held in equilibrium for 20 minutes to extract moisture from the sample. The epoxy moisture content for the 22-sample subset ranged between 0.33% and 1.39% and averaged 0.81%. The histogram for this data is presented in Figure 26.

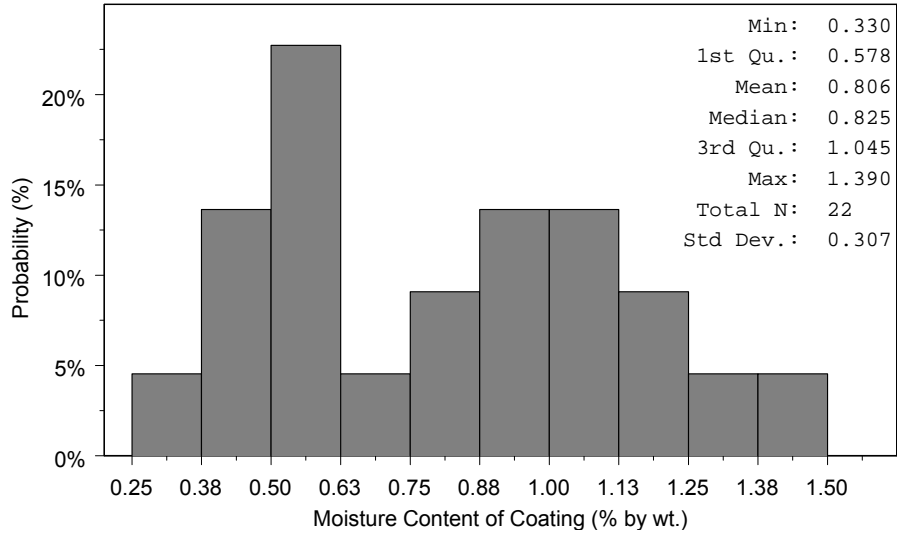
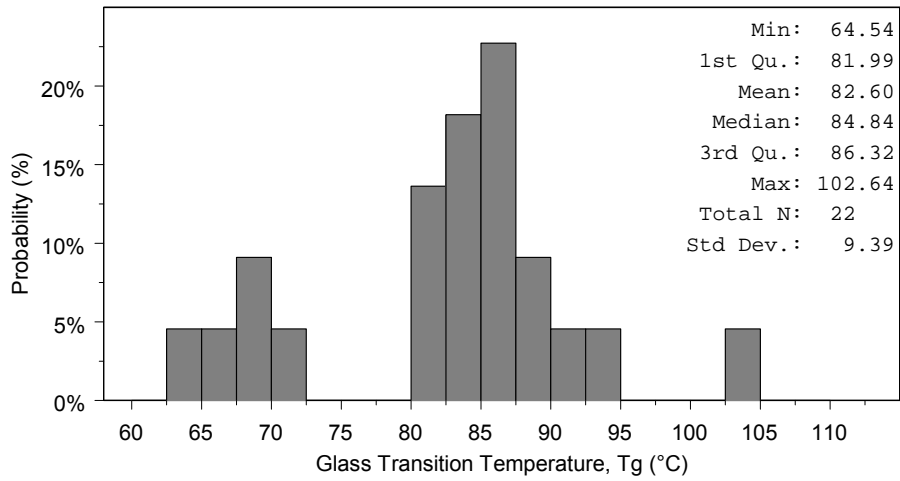


Figure 26 Histogram of Epoxy Coating Moisture Content

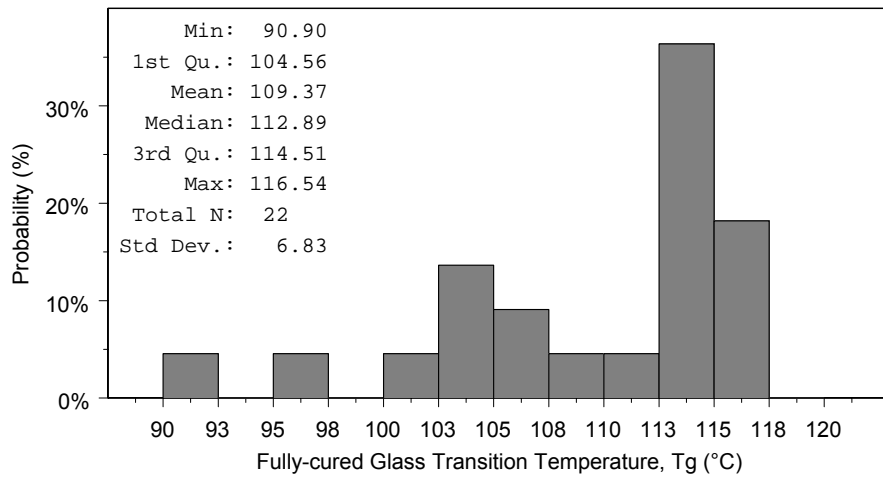
Glass Transition Temperature of Epoxy Coating

A Differential Scanning Calorimeter (DSC) measures the temperature differences between a sample and an inert reference material as the materials are heated at a known rate. Chemical reactions that may result from heating will either give off heat (exotherm) or absorb heat (endotherm). The total energy transferred in or out of the sample can be monitored over time, and this technique can be used to determine the glass transition temperature (T_g) of a thermoset polymer, such as epoxy. The T_g was measured by DSC for a sample of the epoxy coating from each of 22 selected ECR specimens. Results are presented in Table 8. Histograms provided in Figure 27 summarize the initial post-treatment T_g of the coating, the final, fully cured T_g of the coating, and the change in T_g from initial to final for each of the coating samples. The T_g was determined first for the coating in the condition as removed from the concrete after treatment. To determine the initial T_g of the 3.0-gram epoxy samples, the DSC was programmed to equilibrate the temperature at 25.00°C and then increase at 10.00°C/min to 120.00°C. The observed T_g values ranged between 64.54°C and 102.64°C and the average was 82.60°C, as shown in Figure 27a. Then, the samples were placed in an oven for 4 hours at 160.00°C to fully cure the coating. Next, the DSC was programmed to equilibrate at 80.00°C and temperatures were elevated at 10.00°C/min to 160.00°C. The final T_g ranged from 90.90°C to 116.54°C, with an average value of 109.37°C, as shown in Figure 27b.

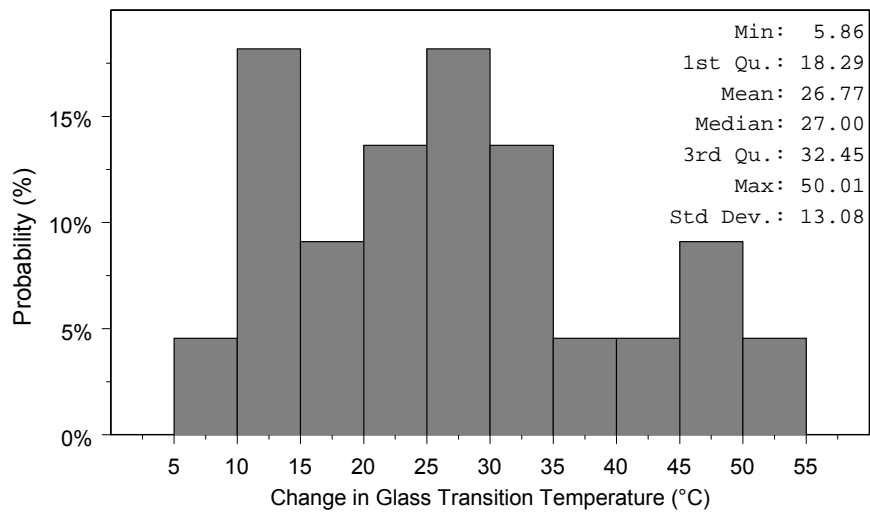
The glass transition temperature of a polymer is controlled by its chemical structure, molecular weight of the polymer chains and the degree of cross-linking (Stevens, M. P., 1999). Consequently, the T_g may, in part, indicate the degree of cure of a polymer. The variance for the initial T_g values was relatively high (CoV = 11.4%, whereas the fully-cured T_g data exhibit lower variance (CoV = 6.2%). This suggests that, once completely cured, the thermal and structural properties of the epoxy coatings are similar to one another, regardless of time of construction and manufacturing conditions of the respective bridges and their constituent materials, and that the coatings, when placed in service, possessed varying degrees of cure. It is important to note that other factors, such as aging due to exposure to ultraviolet light, may alter the structure of the epoxy coating, but the final curing process employed would not remove such variations.



a.)



b.)



c.)

Figure 27 Histograms of Glass Transition Temperature of the Epoxy Coating

The average change in glass-transition temperature (Figure 27c.) was 26.77°C and ranged from 5.86°C to 50.01°C. One might conclude that none of the samples tested had an opportunity to reach full polymerization. Certainly, the extent to which glass transition temperatures changed after extended curing suggests that at least some of the ECR evaluated in this study had not been fully-cured at the time of bridge construction. However, the apparent glass transition temperature of a coating may be directly affected by the presence of moisture within the coating, as observed in this study. Absorbed moisture may exist between the chains of a polymer, and serve as a plasticizer. Upon extended temperature exposure, not only are potential polymerization reactions pushed to completion, but interstitial moisture is also driven from the coating, and both actions serve to increase the T_g . Thus the effects of degree of polymerization and the presence of absorbed moisture cannot be completely differentiated.

Relationships between Moisture, Cracking and Glass Transition Temperatures of Coatings

The moisture content of the coating was compared to change between the initial and final T_g measurements. The correlation was made using the 22 specimens discussed above. The data is presented in Figure 28 and exhibited a correlation coefficient (R^2) of 0.17 and a p-value of 0.053. The relationship suggests that greater moisture absorption corresponds to greater change in T_g after final curing is induced. This is to be expected because lower initial T_g values indicate a lower molecular weight and this provides a greater amount of interstitial (free) volume for a given sample to absorb moisture.

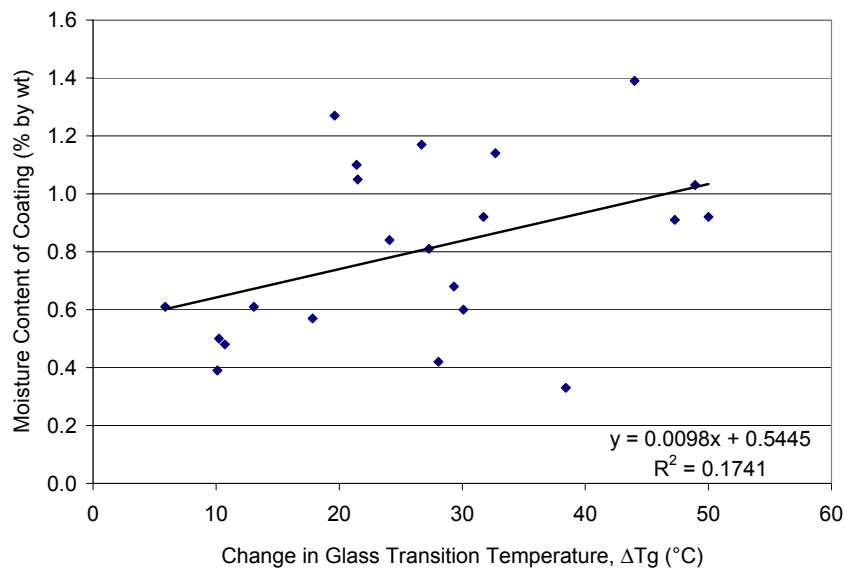


Figure 28 Relationship between Change in Glass transition Temperature and Moisture Content of Coating

Correlation between the crack frequency and the change in T_g are presented in Figure 29. The relationship exhibited a correlation coefficient, R^2 , of 0.44 and a p-value of 0.001. It was found that coating exhibiting a greater change in T_g had a higher likelihood of surface cracking. One might conclude that the epoxy coating will be more prone to damage if it is not fully cured and has absorbed significant moisture.

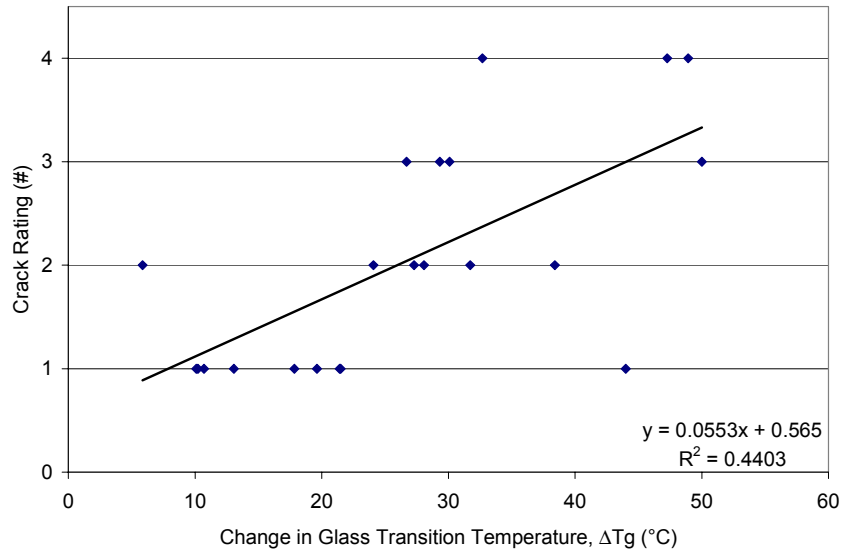


Figure 29 Relationship between Change in Glass Transition Temperature and Crack Rating of Coating

To complete the discussion, the crack ratings of the coatings were finally compared to the moisture content, presumably absorbed from the surrounding concrete while in service. A poor correlation ($R^2=0.04$) was observed, with corresponding p-value of 0.386, suggesting that increased moisture uptake corresponds to greater chance of cracks in the coating surface.

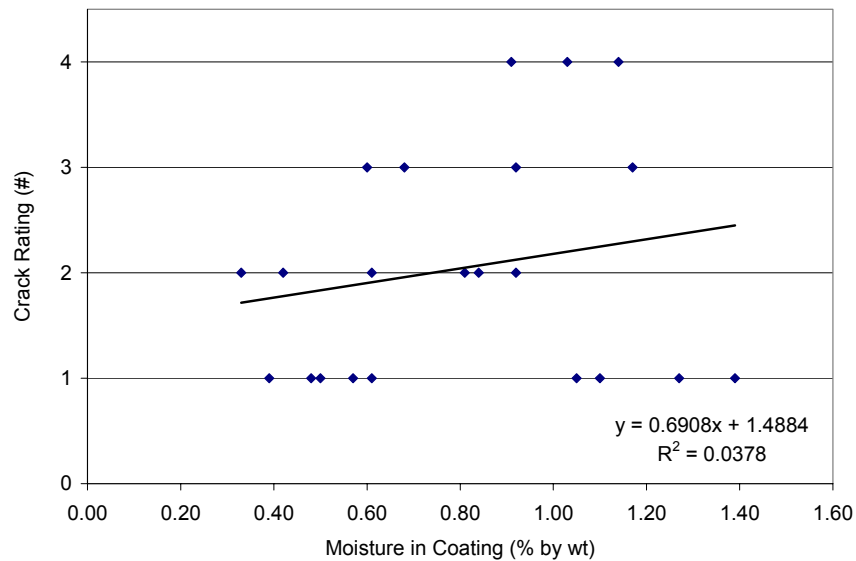


Figure 30 Relationship between Moisture Content and Crack Rating of Coating

Although the observed trends are of interest, the study contained insufficient data to determine the exact cause of the cracking. However, these observations highlight the need for additional evaluation to determine the significance of the micro cracks in the coating surface relative to the overall performance of epoxy coatings for reinforcing steel.

Development of a Probabilistic Model for Corrosion-Related Service Life

Recently, it has been recognized that deterioration of field structures can be better estimated by stochastic modeling based on samples obtained from individual structures or a system of structures, rather than by deterministic models using fixed input values. One such model employs a solution to Fick's Second Law of Diffusion, for one-dimensional diffusion into a semi-infinite slab, to describe the ingress of chloride and the initiation of corrosion for bare steel in concrete bridge decks (Kirkpatrick, T. J. et al., 2002b). The four variables, driving surface concentration, C_o , effective diffusion coefficient, D_c , clear cover depth, x , and the chloride concentration at the bar depth necessary to initiate corrosion, $C_{(x,t)}$, can be represented as distributions, rather than single values for a given structure or system of structures. The distributions can be selected by fitting to measured values obtained from field-testing. Using a statistical re-sampling technique referred to as bootstrap methods, the distribution of each input variable can be implemented into the physical model. Repeated sampling at random from each of the input distributions and calculation of the physical model using these selected inputs results in a distribution for the output value, in this case time to corrosion initiation.

Two specific methods can be used for the selection of input values from the respective distributions. The first, known as the parametric bootstrap method, relies upon proper selection of the probability distribution function that best describes the measured parameter. For the diffusion model, the clear cover depth has been shown previously to conform to a normal distribution, whereas the surface concentration and effective diffusion coefficients appear to conform to gamma distributions. The distribution of the chloride initiation concentration is still uncertain.

The second method of input selection, referred to as a simple bootstrap, circumvents the uncertainties associated with assuming a distribution function. It simply involves direct sampling, at random, from the available measured data for the system in question. The obvious limitation is the number of measurements available for sampling for each input parameter. However, the method has proven successful in predicting life expectancy of bridge decks subject to chloride-induced corrosion, and has been validated against historic bridge performance data in Virginia (Kirkpatrick, T. J. et al., 2002a).

The referenced study, in which the stochastic modeling technique was developed, used field data from individual bridge decks to predict the service life of each deck. In this study, we will consider the distribution of parameters as representative of Virginia's bridge decks as a system of bridge components. Since the study includes structures from interstate, primary, secondary and rural routes, as well as a variety of geographic locations, it is representative of geography and route types of the system of bridges in Virginia (Kirkpatrick, T. J. et al., 2002b). The purpose will be to compare the time to initiation for bare steel and ECR decks, as a system.

Simulation Input Data

The clear cover depths, x , measured in the field were compiled for all 21 bridges surveyed in the phase II study (Pyc, W., 1998), as well as the 3 bridge decks observed in the phase I study (Zemajtis, J. et al., 1997). The eight ECR decks of this phase were a subset of phase II. However, the bare steel decks were unique to this study, and the clear cover depths for those two decks were also incorporated, for a total of 26 decks comprising 2478 observations

ranging from 41 mm to 116 mm. Previous research funded by the Strategic Highway Research Program established a consensus among bridge officials around the country that the level of damage necessitating rehabilitation of a bridge deck is the delamination and spalling, including asphalt patches, of approximately 12% of the surface area of the worst span-lane of a bridge (Fitch, M. G. et al., 1995). Thus, for the system in question, it was determined that the deterioration time should consider the shallowest 12% of cover depths for each of the bridges. Once these first 12% of the bars reach corrosion initiation and propagation, then the deck would be considered to require rehabilitation. Therefore, the distribution of cover depths used in the stochastic models included all measurements less than or equal to the 12th percentile depth for each deck, for a total of 140 observations, which range from 46 mm to 66 mm.

The driving chloride surface concentrations were obtained from acid-soluble chloride concentrations determined from core and powder samples at a depth range of 6 to 19 mm from the surface of the concrete. Previous research has established that chloride concentrations above this elevation are highly variable and fluctuate with time, in regions of deicing salt application. Variations may be due to the effects of wet and dry precipitation cycles, chloride application during the winter season, and chloride leaching during alternate seasons. However, at an elevation of approximately 13 mm below the surface, the driving chloride concentration reaches a maximum, and becomes relatively stable over time (Cady, P. D. & Weyers, R. E., 1983). Thirty-six values were obtained from three bridges in the phase I study, 202 observations gathered from 21 bridges in the phase II study, and 139 observations from the cores in this study, for a total of 377 observations from 26 bridge decks with a range of 0.08 kg/m³ to 10.46 kg/m³.

As discussed previously, effective diffusion coefficients, D_c , were calculated using the one-dimensional solution of Fick's Second Law of Diffusion. Thirty-five values were obtained from powdered concrete chloride profiles obtained in three bridge decks during the phase I study (Weyers, R. E. et al., 1997). In addition, 31 diffusion coefficients were estimated from the powdered concrete chloride profiles of the 10 bridge decks in this study. Finally, 131 effective diffusion coefficients were estimated for cores obtained in this study, based upon the chloride concentrations measured at 13 mm from a top surface in 19 mm above the bar. Approximately four of the latter values, which exceeded 500 mm²/yr, were discarded as outliers. The total number of diffusion coefficients employed was 197, from 13 bridge decks. The diffusion coefficients ranged from 10 mm²/yr to 417 mm²/yr.

The final parameter for the diffusion model, and by far the most controversial and least understood, is the chloride concentration necessary to initiate corrosion. For modeling, values presented in the earlier section on Estimating Chloride Concentration at Reinforcement Depth at Corrosion Initiation (p. 33) were employed. Separate groups of values were developed for bare steel bars and ECR bars. Approximately 17 values representing bare steel and 11 values representing ECR were used to describe the initiation concentration. As previously stated, these results are in agreement with other field studies of structures containing bare steel bar (Glass, G. K. & Buenfeld, N. R., 1997).

Estimating Service Life from Chloride Concentration at Corrosion Initiation

Using the probabilistic technique presented by Kirkpatrick with the simulation data outlined above, the service life probability distribution was projected. Note that, since the 12th

percentile cover depths were used, the output prediction would be the time to reach rehabilitation (defined as corrosion of 12 percent of the system surface area). The C_0 values are indicative of environmental exposures in Virginia, and the D_c parameters are functions primarily of the concrete properties, as well as the age and degree of saturation of the concrete. The $C_{(x,t)}$ used to represent corrosion initiation would be primarily a function of the quality and condition of the coating, where present, the maturity of the passive layer on the steel, and the local environment within the concrete, which affects pH, resistivity, and potential gradients.

For bare steel, all of the input properties appeared to be consistent with previously documented conditions in Virginia bridge decks. Using the simulation, the resulting cumulative distribution of time to corrosion initiation was projected, as shown in Figure 31. The findings indicate that over 50% of Virginia bridge decks constructed with bare steel under specifications in place over the last 20 years are never expected to initiate corrosion, no matter what age they reach. In addition, less than 25% of the decks are projected to initiate corrosion over sufficient area to necessitate rehabilitation within 100 years of construction. Only about 12% of the decks would begin sufficient corrosion to necessitate rehabilitation within the first 34 years. Further, this projection does not consider the propagation period associated with corrosion deterioration, which has been estimated at approximately 3 to 7 years for bare steel decks under continuous corrosion (Weyers, R. E. et al., 1993).

Extending our simulation to ECR, we observed projected time to corrosion on the same order of magnitude, as shown in Figure 32. In this case, over 60% of the reinforcement was found to never be susceptible to corrosion, and only about 21% were expected to corrode within 100 years. Although the average initiation concentration for the ECR was found to be greater, the distribution was also more variable, and those values that are associated with the early deterioration corresponded closely to bare steel. For ECR, the first 12% is expected to initiate within 30 years of construction, which is of the same order as that projected for bare steel.

The fact that time to initiation for some ECR bars is no different than for bare steel should not come as a surprise. It has been clearly established that placement of a perfectly intact coating, without damage or holidays, is impractical (Clear, K. C. et al., 1995). Any bare bar surface at a breach in the coating would be expected to corrode as easily as uncoated steel.

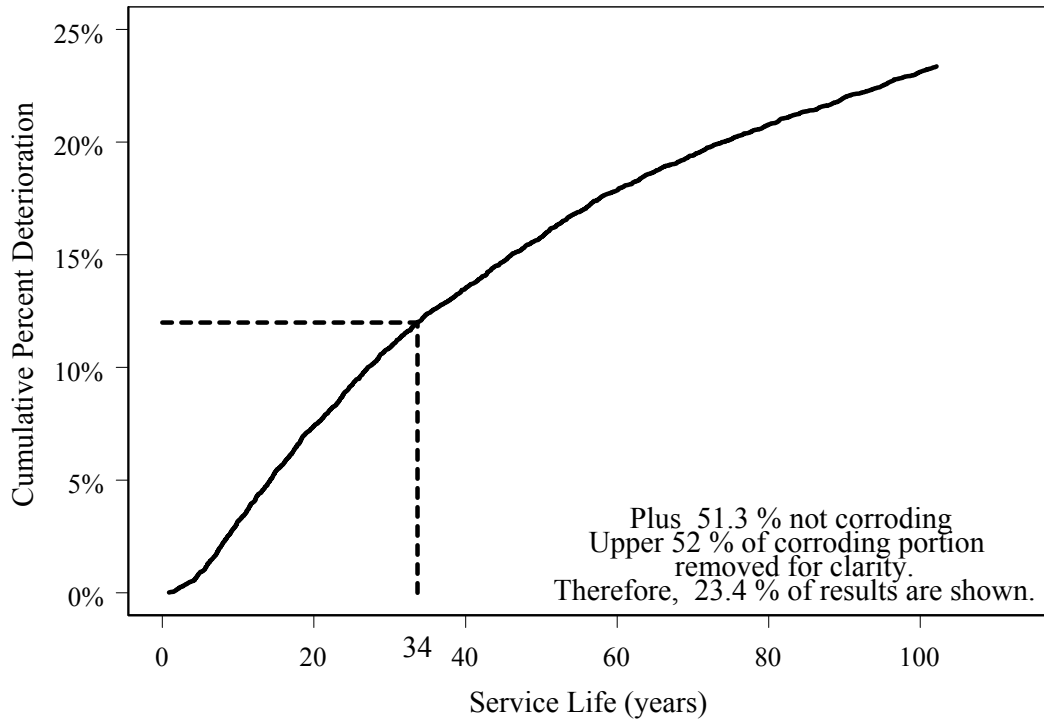


Figure 31 Cumulative Time to Corrosion Initiation for Bare Steel

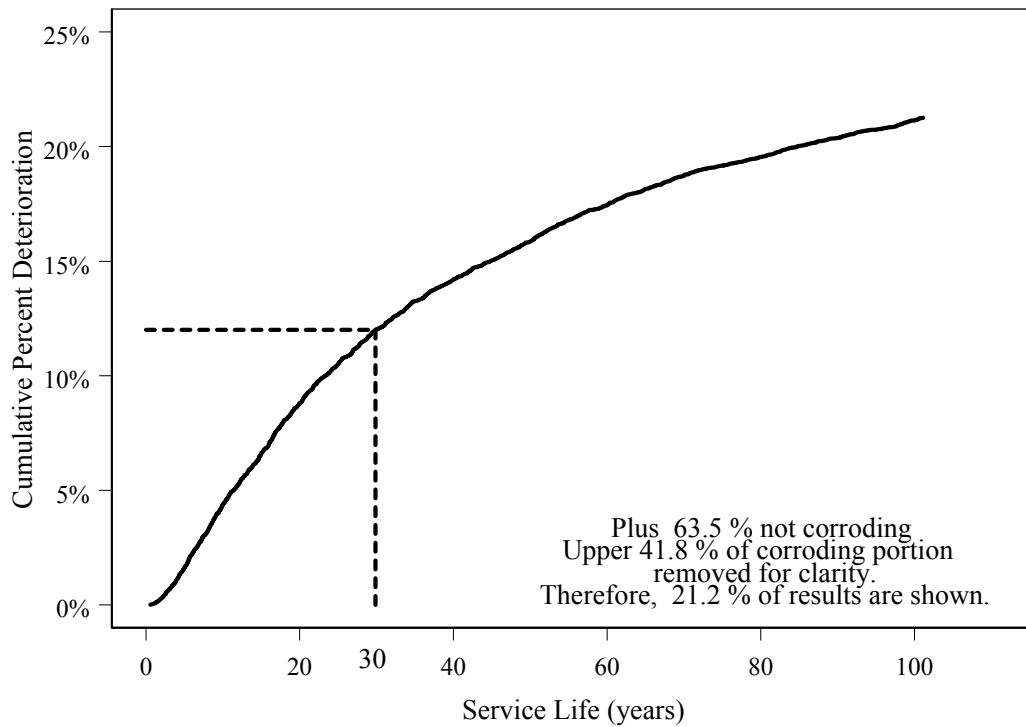


Figure 32 Cumulative Time to Corrosion Initiation for ECR

Estimating Service Life from Chloride Concentration after Cracking

A similar projection was conducted using the chloride contents observed at the time of cracking, rather than at initiation, recognizing that chloride will continue to diffuse into the concrete after corrosion has initiated. Figure 33 and Figure 34 show the projected cumulative probability curves for the first 100 years of service of the population of Virginia bridge decks, based upon chloride measured after cracking in the laboratory specimens. For both bare steel and ECR, the calculation predicted that less than 1 percent of the deck areas in Virginia would reach rehabilitation. This prediction is not at all consistent with experience, and can easily be explained by the accelerated rate of diffusion under laboratory conditions during the test, which allowed chloride to accumulate at the bar during the propagation period much more quickly than would occur in the field. Therefore, projections of service life based directly upon chloride content after cracking were not useful. Thus, the question remained of how to assess the corrosion propagation period for ECR.

Determining Corrosion Rate Ratios of ECR/Bare Steel

Sagüés and others investigated the critical amount of corrosion product necessary to induce cracking, and its relation to the degree of localization of the corrosion anode, where iron-oxide compounds accumulate (Torres-Acosta, A. A., 1999; Sagüés, A. A. et al., 2001). Under the study conditions, the average steel depth lost to corrosion, at the time of cracking, x_{crit} , could be approximated as follows:

$$x_{crit} (mm) \sim 0.011 \left(\frac{x_c}{\Phi} \right) \left(\frac{x_c}{L} + 1 \right)^{1.8} \quad \text{Equation 2}$$

where x_c = clear cover depth (mm)
 Φ = bar diameter (mm)
 L = length of the corroded anode site (mm)
with limits: $(1 \leq x_c/\Phi \leq 7)$ and $(0 \leq x_c/L \leq 3)$

After cracking, bare steel specimens corroded, on average, along approximately 25% of their length, or about 25mm. ECR specimens had corrosion products in 80% of the locations where coating was removed for observation, which translates to an average corrosion length of ~80mm. Using data from the current study, x_{crit} was determined for two cases, the first bare steel and the second ECR, using parameters $x_c = 13\text{mm}$ (0.5 in.), $\Phi = 16\text{mm}$ (#5), and $L = 25\text{mm}$ (1 in.) and 80 mm (3.1 in.), respectively, as follows:

$$\text{Bare: } x_{crit} = 0.011 \left(\frac{13}{16} \right) \left(\frac{13}{25} + 1 \right)^{1.8} = 0.019 \text{ mm}$$

$$\text{ECR: } x_{crit} = 0.011 \left(\frac{13}{16} \right) \left(\frac{13}{80} + 1 \right)^{1.8} = 0.012 \text{ mm}$$

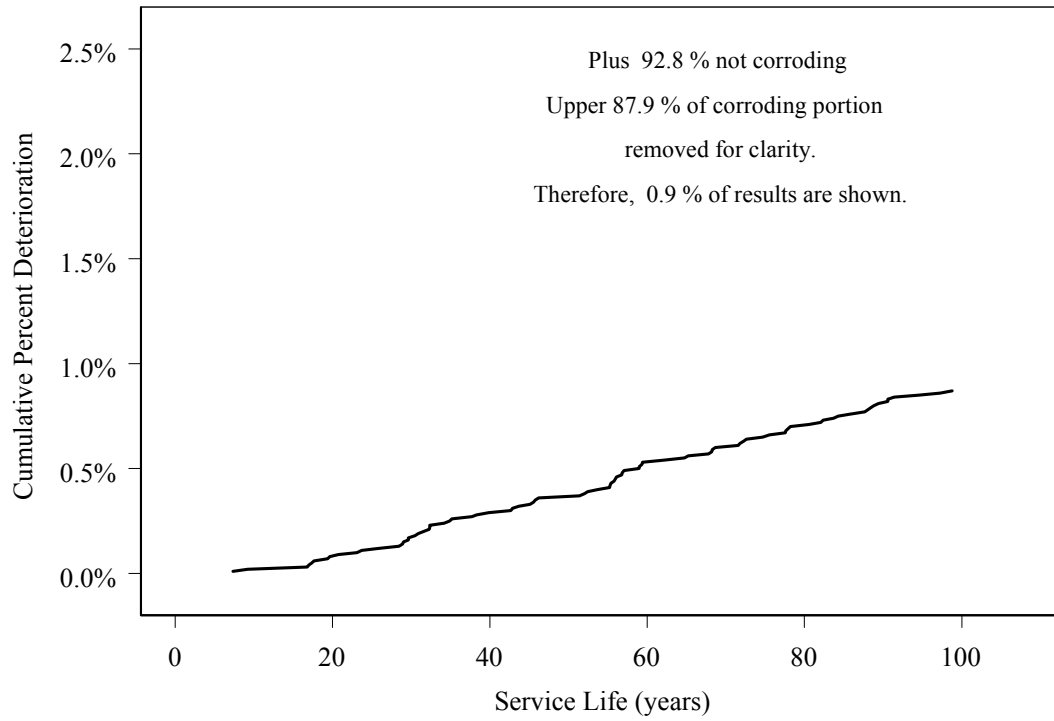


Figure 33 Cumulative Time to Cracking for Bare Steel

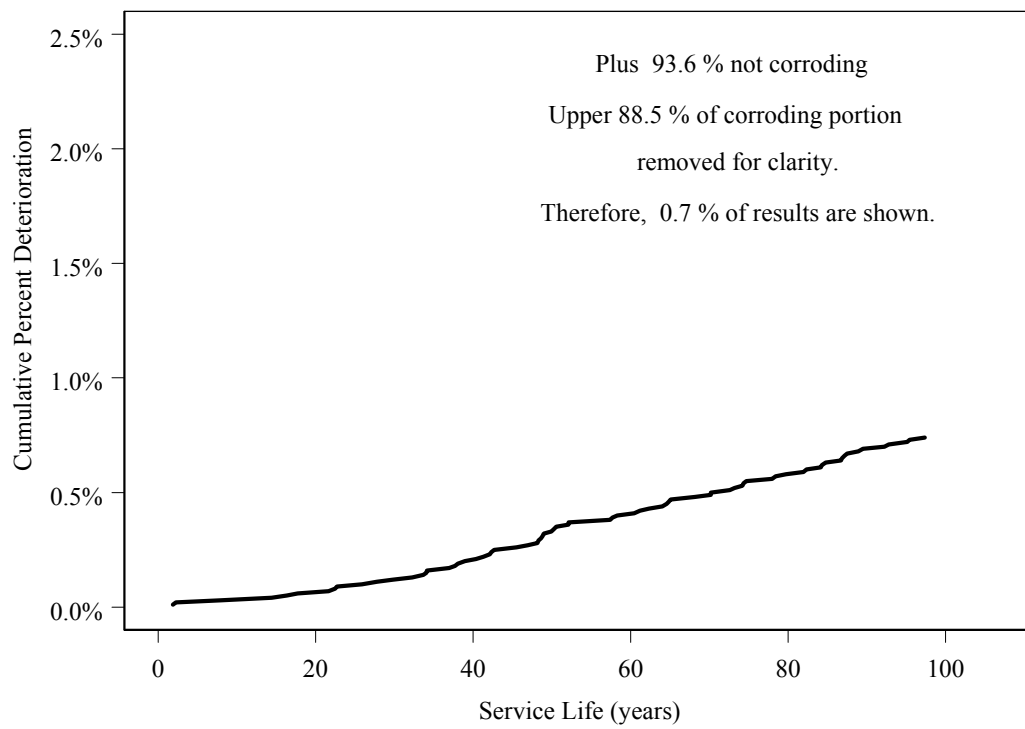


Figure 34 Cumulative Time to Cracking for ECR

Assuming corrosion rate, $C.R.$, is constant with time, Sagüés reasoned that the propagation period, t_p , could be determined by:

$$t_p = C.R. / x_{crit}$$

Equation 3

Using the assumption of constant corrosion rate with time, a proportional comparison of the propagation times during treatment and the calculated x_{crit} for ECR and bare steel resulted in the following estimated relation between corrosion rates of ECR and of bare steel:

$$\frac{t_{p(ECR)}}{t_{p(BARE)}} = \frac{\left(\frac{CR_{(ECR)}}{x_{crit(ECR)}} \right)}{\left(\frac{CR_{(BARE)}}{x_{crit(BARE)}} \right)} = \frac{CR_{(ECR)} \times x_{crit(BARE)}}{CR_{(BARE)} \times x_{crit(ECR)}}$$

Equation 4

$$\frac{CR_{(ECR)}}{CR_{(BARE)}} = \left(\frac{x_{crit(ECR)}}{x_{crit(BARE)}} \right) \left(\frac{t_{p(BARE)}}{t_{p(ECR)}} \right)$$

Thus, substituting experimental values for x_{crit} and t_p revealed the following average proportional rate of corrosion for ECR relative to bare steel:

$$\frac{CR_{(ECR)}}{CR_{(BARE)}} = \left(\frac{0.012}{0.019} \right) \left(\frac{1.28}{0.96} \right) = (0.63)(1.33) = 0.84$$

The corrosion rate ratio of ECR to bare steel at the 2.5 percentile level of laboratory propagation times is as follows:

Given $t_{p(ECR)} = 0.49$; $t_{p(BARE)} = 0.35$ at the 2.5 percentile of propagation times:

$$\frac{C.R._{(ECR)}}{C.R._{(BARE)}} = \frac{t_{(ECR)}}{t_{(BARE)}} \times \frac{x_{crit(ECR)}}{x_{crit(BARE)}} = \left(\frac{0.49}{0.35} \right) \left(\frac{0.012}{0.019} \right) = 0.88$$

Table 9 presents the respective corrosion rate ratios for ECR versus bare steel at selected percentiles of propagation times from the laboratory observations. The average ratio of ECR to bare steel corrosion rates was 0.78, with a standard deviation of 0.093, or coefficient of variation of 12%. Thus, the ratio of corrosion rates has not varied greatly over a range of propagation times.

Table 9 Percentiles of Propagation Times (ECR vs. Bare)

Percentile Propagation Time (%)	Propagation, $t_{p(\text{ECR})}$ (years)	Propagation, $t_{p(\text{BARE})}$ (years)	$t_{p(\text{ECR})} - t_{p(\text{BARE})}$ (years)	Corrosion Rate Ratio $\text{C.R.}_{(\text{ECR})}/\text{C.R.}_{(\text{Bare})}$
2.5	0.49	0.35	0.14	0.88
5.0	0.50	0.46	0.04	0.68
10.0	0.67	0.58	0.09	0.73
12.0	0.68	0.58	0.10	0.73
20.0	0.85	0.61	0.24	0.88
Average:				0.78

Influence of Cover Depth on Laboratory Propagation Time

Sagüés' relation indicates that the degree of corrosion necessary to induce cracking is a function of clear cover depth. Liu performed a study of reinforcing steel in large scale slab specimens subject to various chloride levels, and also determined that cracking was in part a function of clear cover (Liu, Y. & Weyers, R. E., 1998). To project the corrosion propagation period for ECR in a field structure, it is necessary to convert the observed laboratory corrosion rate relationship to account for the greater cover depths in field structures.

The average cover depth in Virginia bridge decks is 65mm, with a standard deviation of 8.9 mm. Thus, the shallowest 2.5 percentile of cover depths are estimated to be less than or equal to 47 mm. The critical penetration depth, x_{crit} , at $x_c = 47\text{mm}$ could be estimated for ECR and bare steel as follows:

$$\text{ECR: } x_{crit} = 0.011 \left(\frac{47}{16} \right) \left(\frac{47}{80} + 1 \right)^{1.8} = 0.074 \text{ mm}$$

$$\text{Bare: } x_{crit} = 0.011 \left(\frac{47}{16} \right) \left(\frac{47}{25} + 1 \right)^{1.8} = 0.217 \text{ mm}$$

Results of similar calculations at selected cover depth percentiles are presented in Table 10.

Table 10 Critical Depth of Penetration for ECR vs. Bare Steel

Percentile of Field Cover Depth (%)	Cover Depth (mm)	$x_{crit(\text{ECR})}$ (mm)	$x_{crit(\text{BARE})}$ (mm)
2.5	47	0.074	0.217
5.0	50	0.082	0.248
10.0	54	0.094	0.294
12.0	55	0.097	0.307
20.0	57	0.103	0.332

Correlation to Field Results

Since the corrosion rate ratios and the corrosion product necessary to induce cracking are based upon accelerated corrosion rates, it is useful to make a comparison to specimens corroded under field conditions. Liu investigated the depth of penetration of bars under field exposures with varying cover depths of 25.4, 50.8, and 76.2 mm (1, 2 and 3 in.)(Liu, Y., 1996).

Considering these cover depths, the predicted critical penetration depths for bare steel, according to Equation 2 would be:

$$25.4 \text{ mm (1 in.): } x_{crit} = 0.011 \left(\frac{25.4}{16} \right) \left(\frac{25.4}{25} + 1 \right)^{1.8} = 0.062 \text{ mm (2.4 mils)}$$

$$50.8 \text{ mm (2 in.): } x_{crit} = 0.011 \left(\frac{50.8}{16} \right) \left(\frac{50.8}{25} + 1 \right)^{1.8} = 0.253 \text{ mm (9.96 mils)}$$

$$76.2 \text{ mm (3 in.): } x_{crit} = 0.011 \left(\frac{76.2}{16} \right) \left(\frac{76.2}{25} + 1 \right)^{1.8} = 0.649 \text{ mm (25.5 mils)}$$

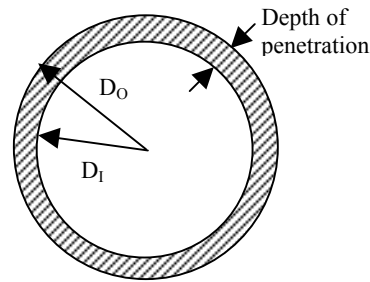
These values are corroborated by the reported findings of Spellman and Stratfull, who indicated that field results showed corrosion penetration depths up to 29 mils (0.736 mm) (Spellman, D. L. & Stratfull, R. F., 1970). Interpretation of results presented by Clear suggested 0.094 mm. Thus, the critical penetration values are consistent with previously reported corrosion penetration depths under field exposures.

Liu presented a physical model to determine the depth of steel penetration by corrosion and its relation to corrosion rate and development of expansive corrosion products (Liu, Y. & Weyers, R. E., 1998). The cross-sectional area, A_c , lost to corrosion, assuming a round bar for simplicity, can be physically related to the depth of penetration as follows:

D_o = outside diameter (prior to corrosion)

D_I = inside diameter (after corrosion)

$x_{crit} = D_o - D_I$ = depth of penetration



$$A_c = \frac{\pi D_o^2}{4} - \frac{\pi D_I^2}{4} = \frac{\pi (D_o^2 - D_I^2)}{4}$$

Equation 5

Multiplying A_c by the density of steel, 7.87 g/cm^3 gives the mass of steel that has been lost to corrosion. As an example, consider the estimated depth of penetration for 25.4 mm (1 in.) cover:

Given $x_c = 25.4 \text{ mm}$; $x_{crit} = 0.062 \text{ mm}$

$$D_I = 15.875 - 0.062 = 15.813 \text{ mm}$$

$$A_{c(BARE)} = \frac{\pi (15.875^2 - 15.813^2)}{4} \times 7.87 \frac{\text{g}}{\text{cm}^3} \times 0.001 \frac{\text{cm}^3}{\text{mm}^3} = 0.303 \text{ g} = 303 \text{ mg}$$

The surface area of the bare steel bar can be estimated as:

$$\pi \times D \times L = (3.14) (1.587 \text{ cm}) (2.5 \text{ cm}) = 12.5 \text{ cm}^2$$

Thus, the weight loss can be normalized to bar length by dividing total mass loss by bar surface area:

$$303 \text{ mg} / 12.5 \text{ cm}^2 = 24.2 \text{ mg/cm}^2$$

Table 11 Projected Mass Loss for Bare Steel

Cover Depth (mm)	D ₁ (mm)	Total Mass Loss (g)	Estimated Mass Loss per Bar Area (mg/cm ²)	Normalized Mass Loss reported by Liu (mg/cm ²)
25.4	15.813	0.303	24.2	29.8
50.4	15.616	1.260	101	39.3
76.2	15.221	3.141	252	60.1

Considering the cover depths of 25.4, 50.8, and 76.2 mm (1, 2 and 3 in.) reported by Liu (Liu, Y., 1996), the normalized mass loss for bare steel is presented in Table 11. The latter two columns contain estimated values as calculated using Equation 2, and the actual values reported by Liu for field exposure specimens, respectively. For shallow depths, less than ~ 50 mm, the normalized mass loss projected using Sagüés' equation were of the same order as those reported by Liu for field specimens. Similar evaluation for ECR, considering a corroded bar length of 80 mm, and corresponding surface area of 39.8 cm², gives the results presented in Table 12.

Table 12 Projected Mass Loss for ECR

Cover Depth (mm)	D ₁ (mm)	Total Mass Loss (g)	Estimated Mass loss per Bar area (mg/cm ²)	Normalized Mass Loss reported by Liu (mg/cm ²)
25.4	15.846	0.455	11.4	29.8
50.4	15.790	1.330	33.4	39.3
76.2	15.699	2.746	68.9	60.1

As it happens, the predicted mass loss values for ECR are in even closer agreement than the bare steel mass loss projections, when compared with those reported by Liu for field exposures. It is possible that the corroded bar sites in Liu's large-scale field specimens were less localized than those in the laboratory cores of this study. Thus, if the values reported by Liu were increased by a factor of 80mm/25mm = 3.2, it is possible to observe closer agreement between the bare steel specimens in this study and the field observations, giving a general agreement between the projected values calculated herein and the field values for cover depths on the order of 51 mm (2 in.), as found in Virginia bridge decks.

Estimating ECR Propagation Time under Field Conditions

Larson and others reported the time from corrosion initiation to cracking for bare steel was approximately 3 to 5 years (Larson, T. D. et al., 1969). Liu and Weyers projected that the field service corrosion damage propagation period for bare steel varies from about 3 to 7 years as

a function of cover depth and assuming a typical corrosion rate for bare steel in field concrete of approximately $1.1 \mu\text{A}/\text{cm}^2$ ($1 \text{ mA}/\text{ft}^2$) corrosion rate (Liu, Y. & Weyers, R. E., 1998; Sagüés, A. A. & Zayed, A. M., 1991). Thus, the field service corrosion propagation period for bare steel, $t_{p(BARE,Field)}$, based upon clear cover depth, can be estimated from Liu and Weyers.

Considering again the relation of corrosion rates and propagation times for ECR and bare steel, as presented in Equation 4, the propagation time for ECR under field exposure can be estimated for various cover depths, using the corrosion rate information determined previously. For example, for the 2.5 percentile cover depth, ($x_{c(2.5\%)} = 47 \text{ mm}$), the bare steel propagation period is approximately 3 years, thus the relative propagation period for ECR can be estimated as follows:

$$\frac{t_{p(ECR)}}{t_{p(BARE)}} = \frac{CR_{(ECR)} \times x_{crit(BARE)}}{CR_{(BARE)} \times x_{crit(ECR)}} = (0.88) \left(\frac{0.217}{0.074} \right) = 2.58$$

$$t_{p(ECR,Field)} = t_{p(BARE,Field)} \times 2.58 = 3.0 \times 2.58 = 8 \text{ years}$$

Subtracting the propagation period for bare steel gives an additional propagation period for ECR of 5 years beyond bare steel.

For the percentiles of cover, as discussed previously, Table 13 presents the expected propagation times for bare steel and ECR, and shows the additional corrosion propagation time provided by ECR, $t_{p(ECR,Field)} - t_{p(BARE,Field)}$, beyond bare steel in field service.

Table 13 Estimated Propagation Times for ECR in Field Service

Percentile (%)	Cover Depth (mm)	$t_{p(BARE,Field)}$ (yr)	C.R. ratio	$t_{p(ECR,Field)}$ (yr)	$t_{p(ECR,Field)} - t_{p(BARE,Field)}$ (yr)
2.5	47	3.0	2.58	8	5
5.0	50	3.5	2.06	7	3
10.0	54	4.0	2.28	9	5
12.0	55	4.0	2.31	9	5
20.0	57	4.5	2.75	12	7
Average		4	2.29	9	5

Thus, the average service life extension contributed by ECR during the corrosion propagation phase can be estimated at 5 years.

Presently no effective method exists for the rehabilitation of concrete bridge components built with ECR. The removal of chloride-contaminated cover concrete is not likely to alleviate corrosion of ECR, once initiated, because the corrosion takes place under the coating. The removal of cover concrete does not remove the chloride from beneath the coating, and does nothing to address the development of an acidic, therefore corrosive, localized environment beneath the coating. In addition, no existing corrosion condition assessment method is amenable to field survey work. Therefore, there are significant but unquantifiable risks in the continued use of ECR as the primary method of corrosion prevention.

Stainless Steel as a Cost-Effective Alternative

Stainless steel is being employed on a limited basis in several states to address corrosion problems in high-chloride environments. As a brief analysis of the cost effectiveness of stainless steel reinforcement as an alternative to ECR, consider the increase in construction costs of stainless steel, compared to black steel or ECR at the present time. In a previous report, the life-cycle costs of corrosion prevention alternatives were discussed, based upon 1997 cost information from the Virginia Department of Transportation.(Pyc, W. A. et al., 2000) Inquiries into the current prices for reinforcement, also to include stainless steel (316LN or Duplex 2205), show that bare steel and ECR prices are more or less the same as previously reported. Table 14 presents the material and installed costs for bare steel, ECR and stainless steel reinforcement (Pianca, F., 2002).

Table 14 Reinforcement Costs

Type	Material Cost Only (\$/lb)	Installed price (\$/lb)
Bare	\$ 0.20	\$ 0.49
ECR	\$ 0.35	\$ 0.62
Stainless Steel	\$ 1.50	\$ 2.36

A typical bridge deck, containing identical top and bottom mats, with #5 (16 mm) primary reinforcement at approximate 200 mm (8 in.) centers and 13-mm diameter (#4) temperature/shrinkage reinforcement at 300 mm (12 in.) centers, contains approximately 5 pounds of reinforcement per square foot.

Both the material costs and the installed cost for this "model" bridge deck can thus be projected, and the differences in costs versus bare steel estimated, as shown in Table 15. The price of a concrete overlay, including milling, patching, and traffic control, for a deck which reaches rehabilitation prior to the 75-year design life was estimated at \$10.38 per square foot in 1995 (Pyc, W. A. et al., 1998). Using an effective annual inflation rate of 2.13% from 1995 to present, as determined from both construction cost and general U.S. inflation indices, the estimated current cost of this overlay would be \$12.03 (McCusker, J. J., 2002; Engineering News-Record, 2002). Thus, the additional cost for stainless steel reinforcement, \$9.35 per square foot more than bare steel and \$8.70 per square foot more than ECR, is less than the cost of one concrete overlay, including traffic control costs.

Table 15 Unit Costs for Deck Reinforcement

Type	Material Only		Installed	
	Unit Cost (\$/ft ²)	Cost Increase over Bare (\$/ft ²)	Unit Cost (\$/ft ²)	Cost Increase over Bare (\$/ft ²)
Bare	\$ 1.00	-	\$ 2.45	-
ECR	\$ 1.75	\$ 0.75	\$ 3.10	\$ 0.65
Stainless Steel	\$ 7.50	\$ 6.50	\$ 11.80	\$ 9.35

It is important to note that stainless steel reinforcement, though a proven prevention method, has not yet come into common use, and therefore, has yet to reach fair market value

(McDonald, D. B. et al., 1998). As its use increases, economies of scale and competition in the market can be expected to reduce prices, in much the same manner as occurred with ECR during its initial implementation (Manning, D. G., 1996). A significant portion of the in-place cost of stainless steel reinforcement is reported to be associated with the "fixtures," such as chairs, tie-wire, and conduits. Many specifications require that such ancillary items also be composed of stainless steel, thus driving up the current in-place cost. As stainless steel reinforcement becomes more common, it is likely that the price premium associated with its use will decrease.

A previous report evaluated the service lives and life cycle costs associated with a number of construction alternatives for reinforced concrete bridge decks (Pyc, W. A. et al., 2000). Using price data from Virginia Department of Transportation, the relative service lives and life cycle costs of ECR with normal Class A4 bridge deck concrete was compared with that of low permeability concrete. Using prices presented in that report, adjusting for inflation at an annual rate of 2.13%, comparisons can be made regarding the cost-effectiveness of corrosion prevention alternatives.

The time to corrosion initiation of bare steel and ECR can be determined from Figure 31 and Figure 32, respectively, for selected percentiles of bridge deck area throughout Virginia. Using the propagation periods calculated for bare steel and ECR, service life predictions and times of rehabilitative overlay activities can be projected for alternative corrosion prevention systems. Consider three reinforcement bar alternatives, all employing low-permeability concrete: bare steel, ECR, and stainless steel (316LN). Low-permeability concrete has been found to extend the time to corrosion initiation by approximately 18 years beyond that of conventional A4 bridge deck concrete (Kirkpatrick, T. J. et al., 2002b). A rehabilitative concrete overlay in Virginia lasts an average of 24 years before further rehabilitation is required (Pyc, W. A. et al., 2000). Table 16 presents the expected rehabilitation times for each deck system at various corrosion probability levels in Virginia.

Table 16 Rehabilitation Times of Corrosion Prevention Systems

Corrosion Percentile (%)	Age(s) at Rehabilitation (yrs)			Number of Overlays Required		
	Bare	ECR	SS	Bare	ECR	SS
5	38,62	43,67	-	2	2	0
10	50	55	-	1	1	0
15	75	80	-	0	0	0
20	98	103	-	0	0	0

Therefore, the cumulative costs over the 75-year life of a structure, including initial construction and rehabilitation with traffic control for the various options can be estimated, as shown in Table 17. The total expenditure is the sum of the initial costs, plus the overlay costs at the rehabilitation age(s) using an annual inflation rate of 2.13%.

From the viewpoint of total expenditures over a 75-year service life, Table 17 shows that ECR is never a cost-effective corrosion prevention alternative in Virginia bridge decks. The only way that ECR could be cost-effective is if it prevents the need for an overlay, as compared to bare steel. For the greatest chloride exposure conditions in Virginia, it is clear that stainless steel is a least-cost alternative.

Table 17 Total Expenditures for Corrosion Prevention Systems

Corrosion Percentile (%)	A4-LPC Concrete (in 2002) (\$/sf)	Reinforcement Installed Price (in 2002)			Overlay w/ traffic control (in 2002) (\$/sf)	Total Expenditure over Life of the Deck*		
		Bare (\$/sf)	ECR (\$/sf)	SS (\$/sf)		Bare (\$/sf)	ECR (\$/sf)	SS (\$/sf)
5	10.25	2.45	3.10	11.80	12.03	83.92	92.51	22.05
10	10.25	2.45	3.10	11.80	12.03	47.23	51.73	22.05
15	10.25	2.45	3.10	11.80	12.03	12.70	13.35	22.05
20	10.25	2.45	3.10	11.80	12.03	12.70	13.35	22.05

* Does not include routine inspection and minor maintenance costs

As shown in Table 15, ECR adds approximately \$0.65 per square foot to the installed price of reinforcement in a typical conventionally reinforced bridge deck. The associated direct savings would be \$65,000 for each 100,000 square feet of bridge deck constructed. During the past three years, VDOT has constructed approximately 1.3 million square feet of bridge decks per year. Deleting the requirement for ECR would save approximately \$845,000 per year.

Benefits versus Risks of Corrosion Prevention Methods

Items considered in evaluating the cost effectiveness of current or proposed solutions generally include initial construction costs and projected maintenance costs. However, such evaluations should also consider the influence of the prevention method in question on future maintenance and rehabilitation options. Is there a greater risk involved in adopting a corrosion prevention strategy for which the benefit is not clearly quantified, and the costs and difficulties involved in mitigating it, should it not perform, are even less well understood?

Findings regarding projected time-to-corrosion for decks containing bare steel suggest that the severity of the corrosion-related deterioration issue has been overestimated, at least for Virginia bridge decks. Interestingly, a summary of Virginia records indicated that, as of 1998, more than 42% of bridge decks in service had been built prior to 1950, indicating a significant number of structures built under less stringent concrete and cover parameters were still performing adequately (Kerley, M., 1998). Of course, this data does not indicate whether overlays or other rehabilitation had been undertaken to extend lifespan. However, recent analysis showed that 25% of bridge decks built about 30 years ago (1968-1972) have received a maintenance overlay (polymer concrete) and only 13% had received a concrete overlay (Kirkpatrick, T. J. et al., 2002a). Conversely, records do not indicate whether bridges taken out of service were the result of corrosion related deterioration, other structural deterioration, or functional obsolescence.

With an additional increase in cover requirement, improved concrete specifications, and more recently, the adoption of high-performance, low permeable concretes to prevent alkali-silica reaction, the threat due to reinforcement corrosion in Virginia bridge decks appears to be limited to regions of intense salt usage, which can be correlated to both regional weather patterns and traffic volume (Dadson, D. K., 2001). Within Virginia, the areas of highest risk appear to be in the Northern Virginia, Culpeper and Staunton Engineering Districts, in locations with higher than average traffic counts, where deicing operations due to inclement winter weather are more common and more intense.

At present, federal guidelines require the use of a corrosion prevention method in bridge deck construction. Currently, ECR is the most widely accepted method. Best estimates have shown that ECR is not cost effective in Virginia bridge decks. A more prudent approach to application of limited highway construction and maintenance funds would be to differentiate between regions or structures based on severity of environment and traffic exposure. Structures in less severe exposures are sure to benefit from improvements in concrete quality and increased cover depth, whereas high risk areas might be more effectively addressed on a case-by-case basis, by implementing a more reliable method, such as stainless steel reinforcement.

CONCLUSIONS

Service Life Extension of ECR

In approximately the worst 20% of cases where performance is most critical, ECR provided no significant increase in projected time to corrosion initiation over that of bare steel. For a 100-year lifespan, ECR reduced the proportion of Virginia bridge deck areas expected to corrode by less than 2.5%. Comparing the expected field propagation periods of bare steel and ECR, service life was extended by approximately 5 years using ECR.

The 5-year service life extension estimated in this study is in agreement with a previous study (Weyers, R. E. et al., 1997). The 5-year service life extension provided by ECR is not a cost-effective corrosion protection method for bridge decks in Virginia.

Significance of Increased Chloride Penetration at Cracks

Most cracks in Virginia bridge decks are less than 0.30 mm in surface width, and longitudinal cracking was more commonly observed than transverse cracks. A relatively small number of visible cracks in bridge decks extend to the depth of reinforcement, and no apparent relation exists between crack width and crack depth. Although at early ages the presence of cracks appears to increase the chloride concentration at 19 mm depth by an average of 0.61 kg chloride per cubic meter of concrete in about 61% of cracks, the effect appears to decline with age. As a worst-case condition, bridge deck cracking in Virginia may decrease the time to first repair, but will not significantly reduce the bridge deck service life. This conclusion is based upon observations for the set of 10 subject bridges. Further study of this issue is currently underway.

RECOMMENDATIONS

For critical structures, such as those structures on interstates and U.S. routes in the Northern Virginia, Staunton, and Culpeper districts and other locations with a high rate of deicer salt usage, the use of stainless steel (316LN) reinforcing bar is recommended as the bridge deck corrosion protection system. The use of stainless steel (316LN) reinforcing steel is also recommended for coastal substructures. This report has demonstrated that the additional cost of stainless steel reinforcement is less than the cost of a single rehabilitative overlay for a bridge deck that does not reach 75-year design life. Stainless steel reinforcement may be implemented selectively for decks subject to the most severe exposures. Since 75% of structures are predicted not to reach the chloride corrosion concentration threshold during their expected life, low-

permeability concrete (<1500 coulomb per ASTM C 1202-97) is recommended for all other structures at this time.

Further investigation of the effects of recent specification changes, such as the adoption of pozzolanic admixtures and high-performance, low-permeability concretes, may help in identifying the critical exposures and allow targeted application of more rigorous corrosion control in locations where they are most needed.

Based on observations in this work, future research would be desirable in characterizing the field condition of ECR decks. Electrochemical impedance is not readily applicable to field structures, due to the complexity of the results and the myriad uncertainties concerning the observed systems. Therefore, development of simplified field condition assessment for ECR systems, to be employed by bridge officials in assessing service life and rehabilitation schedules, is still needed.

In addition, it is apparent that at least some of the existing ECR decks in service will not achieve the anticipated design life. Repair procedures and remediation strategies must be specifically developed to address ECR. Some procedures, such as cathodic protection, may not be successfully implemented in such structures. Removing chloride contaminated concrete and installing overlays above ECR that has initiated corrosion may prove insufficient, since corrosion beneath the coating may progress under completely different mechanisms once initiated.

REFERENCES

- ASTM, C 1152-90, Standard Test Method for Acid-Soluble Chloride in Mortar and Concrete, *ASTM Annual Book of ASTM Standards*, v. 04.02 Concrete and Aggregates, 1990.
- ASTM, C 876-91, Standard Test Method for Half-Cell Potentials of Uncoated Reinforcing Steel in Concrete, *ASTM Annual Book of ASTM Standards*, v. 04.02 Concrete and Aggregates, 1991.
- ASTM, C 642-97, Standard Test Method for Density, Absorption, and Voids in Hardened Concrete, *ASTM Annual Book of ASTM Standards*, v. 04.02 Concrete and Aggregates, 1997.
- ASTM, C 702-98, Standard Practice for Reducing Samples of Aggregate to Testing Size, *ASTM Annual Book of ASTM Standards*, v. 04.02 Concrete and Aggregates, 1998.
- ASTM, A 775/A 775M - 01, Standard Specification for Epoxy-Coated Steel Reinforcing Bars, *ASTM Annual Book of ASTM Standards*, v. 01.05 Steel Reinforcement, 2001.
- Atimay, E. and Ferguson, P. M., Early Chloride Corrosion of Reinforcing - A Test Report, *Materials Performance*, v. 13, n. 12, 1974, pp. 18-21.
- Babaei, K. and Hawkins, N. M., Evaluation of Bridge Deck Protective Strategies, *Concrete International*, v. 10, n. 12, 1988, pp. 56-66.
- Beeby, A. W., Corrosion of Reinforcing Steel in Concrete and Its Relation to Cracking, *The Structural Engineer (London)*, v. 56A, n. 3, 1978, pp. 77-81.

- Brown, M. C., Weyers, R. E., and Sprinkel, M. M., Effect of Corrosion-Inhibiting Admixtures on Material Properties of Concrete, *ACI Materials Journal*, v. 98, n. 3, 2001, pp. 240-250.
- Brown, M. C., *Corrosion Protection Service Life Of Epoxy Coated Reinforcing Steel In Virginia Bridge Decks*, Dissertation in Civil and Environmental Engineering, Virginia Polytechnic Institute & State University, Blacksburg, VA, 2002. <http://scholar.lib.vt.edu/theses/available/etd-05132002-120642/>.
- Bureau of Transportation Statistics (BTS), National Transportation Statistics 1999, U.S. Department of Transportation, Washington, D.C., 2000.
- Cady, P. D., Corrosion of Reinforcing Steel in Concrete - A General Overview of the Problem, Tonini, D.E. and Dean, S.W., *Chloride Corrosion of Steel in Concrete*, v. STP 629, p. 3-11. ASTM, Philadelphia, PA, ASTM. 1977.
- Cady, P. D. and Weyers, R. E., Chloride Penetration and the Deterioration of Concrete Bridge Decks, *Cement, Concrete and Aggregates*, v. 5, n. 2, 1983.
- Clear, K. C., Hartt, W. H., McIntyre, J., and Lee, S. K., *Performance of Epoxy-Coated Reinforcing Steel in Highway Bridges*, Report 370, National Academy Press, Washington, D.C., 1995.
- Clear, K. C., Effectiveness of epoxy-coated reinforcing steel, *Concrete International*, v. 14, n. 5, 1992, pp. 58,60-62.
- Covino, B. S., Cramer, S. D., Holcomb, G. R., Russell, J. H., Bullard, S. J., Dahlin, C., and Tinnea, J. S., *Performance of Epoxy-Coated Steel Reinforcement in the Deck of the Perley Bridge*, U.S. Dept. of Energy, Albany, OR, 2000.
- Dadson, D. K., *Impact of Environmental Classification on Steel Girder Bridge Elements Using Bridge Inspection Data*, Dissertation in Civil and Environmental Engineering, Virginia Polytechnic Institute & State University, Blacksburg, VA, 2001, <http://scholar.lib.vt.edu/theses/available/etd-05182001-144700/>.
- Diamond, S., Effects of Two Danish Flyashes on Alkali Contents of Pore Solutions of Cement-Flyash Pastes, *Cement and Concrete Research*, v. 11, 1981, pp. 383-394.
- Engineering News-Record, Construction Cost Index History (1908-2002), McGraw Hill Construction, New York, New York, 2002. <http://enr.construction.com/features/conEco/costIndexes/constIndexHist.asp>. Accessed April 15, 2002.
- Fanous, F. S., Wu, H., and Pape, J., *Impact of Deck Cracking on Durability*, CTRE Management Project 97-5, Center for Transportation Research and Education, Iowa State University, Ames, IA, 2000.
- Fitch, M. G., Weyers, R. E., and Johnson, S. D., Determination of End of Functional Service Life for Concrete Bridge Decks, *Transportation Research Record* n. 1490, 1995, pp. 60-66.

- Glass, G. K. and Buenfeld, N. R., Presentation of the Chloride Threshold Level for Corrosion of Steel in Concrete, *Corrosion Science*, v. 39, n. 5, 1997, pp. 1001-1013.
- Kerley, Malcolm. Personal Communication with Richard E. Weyers, 6 April 1998.
- Kirkpatrick, T. J., *Impact of Specification Changes on Chloride Induced Corrosion Service Life of Virginia Bridge Decks*, Master's Thesis in Civil and Environmental Engineering, Virginia Polytechnic Institute and State University, Blacksburg, VA, 2001, <http://scholar.lib.vt.edu/theses/available/etd-07192001-114248/>.
- Kirkpatrick, T. J., Weyers, R. E., Anderson-Cook, C. M., Sprinkel, M. M., Impact of Specification Changes on Chloride Induced Corrosion Service Life of Bridge Decks, *Cement and Concrete Research*, v. 32, n. 8, 2002a, pp. 1189-1198.
- Kirkpatrick, T. J., Weyers, R. E., Anderson-Cook, C. M., Sprinkel, M. M., Probabilistic Model for the Chloride Induced Corrosion Service Life of Bridge Decks, *Cement and Concrete Research*, v. 32, n. 12, 2002b, pp. 1934-1960.
- Kranc, S. C., Sagüés, A. A., and Presuel-Moreno, F. J., Decreased Corrosion Initiation Time of Steel in Concrete due to Reinforcing Bar Obstruction of Diffusional Flow, *ACI Materials Journal*, v. 99, n. 1, 2002, pp. 51-53.
- Krauss, P. D. and Rogall, E. A., *Transverse Cracking in Newly Constructed Bridge Decks*, NCHRP Report 380, Transportation Research Board, Washington, D.C., 1996.
- Larson, T. D., Cady, P. D., and Theisen, J. C., *Durability of Bridge Deck Concrete*, Pennsylvania State University, State College, PA, 1969.
- Liu, Youping, *Modeling the Time-to-Corrosion Cracking of the Cover Concrete in Chloride Contaminated Reinforced Concrete Structures*, Dissertation in Civil and Environmental Engineering, Virginia Polytechnic Institute & State University, Blacksburg, VA, 1996, <http://scholar.lib.vt.edu/theses/available/etd-44541620119653540/>.
- Liu, Y. and Weyers, R. E., Modeling the Time-to-Corrosion Cracking in Chloride Contaminated Reinforced Concrete Structures, *ACI Materials Journal*, v. 95, n. 6, 1998, pp. 675-681.
- Lorentz, T. and French, C., Corrosion of Reinforcing Steel in Concrete: Effects of Materials, Mix Composition, and Cracking, *ACI Materials Journal*, v. 92, n. 2, 1995, pp. 181-190.
- Manning, D.G., Corrosion Resistant Design of Concrete Structures, *Proceedings of the Canadian Structural Concrete Conference*, University of Toronto, 1981, pp. 199-223.
- Manning, D.G., Corrosion Performance of Epoxy-Coated Reinforcing Steel: North American Experience, *Construction and Building Materials*, v. 10, n. 5, 1996, pp. 349-365.
- Martin, H. and Schiessl, P., The Influence of Cracks on the Corrosion of Steel in Concrete, *International Symposium on the Durability of Concrete*, RILEM, v. 2, 1962.

- Matsushima, M. et al., A Study of the Application of Reliability Theory to the Design of Concrete Cover, *Magazine of Concrete Research*, v. 50, n. 1, 1998, pp. 5-16.
- McDonald, D. B., Pfeifer, D. W., and Sherman, M. R., *Corrosion Evaluation of Epoxy-Coated, Metallic-Clad and Solid Metallic Reinforcing Bars in Concrete*, FHWA-RD-98-153, National Technical Information Services, Springfield, Virginia, 1998.
- McCusker, J. J., What Was the Inflation Rate Then?, Economic History Services, 2001, <http://www.eh.net/hmit/inflation/>. Accessed April 15,2002.
- Pianca, Frank. Personal Communication with Richard E. Weyers, 15 April 2002.
- Pyc, W. A., Weyers, R. E., and Sprinkel, M. M., *Corrosion Protection Performance of Corrosion Inhibitors and Epoxy-Coated Reinforcing Steel in a Simulated Concrete Pore Water Solution*, VTRC 98-R42, Virginia Transportation Research Council, Charlottesville, Virginia, 1998.
- Pyc, W A, Weyers, R E, Weyers, R M, Mokarem, D W, Zemajtis, J, Sprinkel, M M, and Dillard, J G, *Field Performance of Epoxy-Coated Reinforcing Steel in Virginia Bridge Decks*, VTRC 00-R16, Virginia Transportation Research Council, Charlottesville, VA, 2000.
- Pyc, Wioleta, *Field Performance of Epoxy-Coated Reinforcing Steel in Virginia Bridge Decks*, Dissertation in Civil and Environmental Engineering, Virginia Polytechnic Institute & State University, Blacksburg, VA, 1998, <http://scholar.lib.vt.edu/theses/available/etd-102998-190256/>.
- Raphael, M. and Shalon, R., A Study of the Influence of Climate on Corrosion and Reinforced Concrete, Proceedings, *RILEM Symposium on Concrete and Reinforced Concrete in Hot Climates*, 1971, pp. 77-96.
- Rieger, Philip H., *Electrochemistry*, 2nd ed., Chapman & Hall, New York & London, 1994.
- Sagüés, A. A., Lee, J.B., Chang, X., Pickering, H., Nystrom, E., Carpenter, W., Kranc, S.C., Simmons, T., Boucher, B., and Hierholzer, S., *Corrosion of Epoxy-Coated Rebar in Florida Bridges*, Final Report to Florida DOT, WPI No. 0510603, University of South Florida, Tampa, FL, 1994.
- Sagüés, A. A., Kranc, S. C., Presuel-Moreno, F., Rey, D., Torres-Acosta, A., and Yao, L., *Corrosion Forecasting for 75-Year Durability Design of Reinforced Concrete*, Florida Department of Transportation, Report BA502, University of South Florida, Tampa, FL, 2001.
- Sagüés, A.A. and Zayed, A.M., Low-Frequency Electrochemical Impedance for Measuring Corrosion of Epoxy-Coated Reinforcing Steel in Concrete, *Corrosion*, v. 47, n. 11, 1991, pp. 852-859.

- Scantlebury, J. D. and Sussex, G. A. M., Impedance Techniques for the Study of Organic Coatings, *Corrosion Control by Organic Coatings*, Leidheiser, H., Jr., Ed., National Association of Corrosion Engineers, Houston, TX, 1981, pp. 51-55.
- Schiessl, P. and Raupach, M., Laboratory Studies and Calculations on the Influence of Crack Width on Chloride-Induced Corrosion of Steel in Concrete, *ACI Materials Journal*, v. 94, n. 1, 1997, pp. 56-62.
- Smith, J. L. and Virmani, Y. P., *Materials and Methods for Corrosion Control of Reinforced and Prestressed Concrete Structures in New Construction*, Report No. FHWA-RD-00-81, Federal Highway Administration, McLean, VA, 2000.
- Spellman, D.L. and Stratfull, R.F., Chlorides and Bridge Deck Deterioration, *Highway Research Record*, n. 328, 1970, pp. 38-49.
- Standish, J. V. and Leidheiser, H., Jr., Properties and Behavior of Corrosion-Protective Organic Coatings As Determined by Electrical Impedance Measurements, *Corrosion Control by Organic Coatings*, Leidheiser, H., Jr., Ed., National Association of Corrosion Engineers, Houston, TX, 1981, pp. 38-44.
- Stratfull, R. F., Jurkovich, W. J., and Spellman, D. L., Corrosion Testing of Bridge Decks, *Transportation Research Record*, n. 539, 1975, pp. 50-59.
- Torres-Acosta, A. A., *Cracking Induced by Localized Corrosion of Reinforcement in Chloride Contaminated Concrete*, Dissertation in Civil and Environmental Engineering, University of South Florida, Tampa, FL, 1999.
- Tremper, B., The Corrosion of Reinforcing Steel in Cracked Concrete, *ACI Journal*, v. 43, n. 10, 1947, pp. 1137-1144.
- Vassie, P., Reinforcement Corrosion and the Durability of Concrete Bridges, *Proceedings of the Institution of Civil Engineers (London)*, v. 76, pt. 1, 1984, pp. 713-723.
- Virginia Department of Highways and Transportation, *Road and Bridge Specifications*, 1978.
- Virginia Department of Highways and Transportation, *Road and Bridge Specifications*, 1982.
- Virginia Department of Transportation, *Road and Bridge Specifications*, 1987.
- Virginia Department of Transportation, *Road and Bridge Specifications*, 1991.
- Weyers, R. E., Prowell, B. D., Sprinkel, M. M., and Vorster, M., *Concrete Bridge Protection, Repair, and Rehabilitation Relative to Reinforcement Corrosion: A Methods Application Manual*, SHRP-S-360, Strategic Highway Research Program - National Research Council, Washington, D.C., 1993.
- Weyers, R. E., *Protocol for In-Service Evaluation of Bridges with Epoxy-Coated Reinforcing Steel*, NCHRP 10-37B, Transportation Research Board, Washington, D.C., 1995.

Weyers, R. E., Sprinkel, M. M., Pyc, W., Zemajtis, J., Liu, Y., and Mokarem, D. W., *Field Investigation of the Corrosion Protection Performance of Bridge Decks and Piles Constructed with Epoxy-Coated Reinforcing Steel in Virginia*, VTRC 98-R4, Virginia Transportation Research Council, Charlottesville, VA, 1997.

Zemajtis, J., Weyers, R. E., and Sprinkel, M. M., *Performance Evaluation of Epoxy-Coated Reinforcing Steel*, VTRC 99-CR2, Virginia Transportation Research Council, Charlottesville, VA, 1997.